An Assessment of the Ozone Loss During the 1999-2000 SOLVE/ THESEO 2000 Arctic Campaign

Mark R. Schoeberl, Paul A Newman, Leslie R. Lait, Thomas J. McGee, John F. Burris
NASA Goddard Space Flight Center
Greenbelt, Md.

Edward V. Browell and William B. Grant
NASA Langley Research Center
Hampton, Va..

Eric C. Richard
NOAA Aeronomy Laboratory
Boulder, Colorado

Peter von der Gathen
Alfred Wegener Institute of Polar and Marine Research
Potsdam, Germany

Richard Bevilacqua
Naval Research Laboratory
Washington,D.C.

Ib S. Mikkelsen
Danish Meteorological Institute
Copenhagen, Denmark

M. J. Molyneux
The Met. Office
Workingham
U. K.

Abstract

Ozone observations from ozonesondes, the lidars aboard the DC-8, in situ ozone measurements from the ER-2, and satellite ozone measurements from Polar Ozone and Aerosol Measurement III (POAM) were used to assess ozone loss during the Sage III Ozone Loss and Validation Experiment (SOLVE) and Third European Stratospheric Experiment on Ozone (THESEO) 1999-2000 Arctic campaign. Two methods of analysis were used. In the first method a simple regression analysis of the data time series is performed on the ozonesonde and POAM measurements within the vortex. In the second method, the ozone measurements from all available ozone data were injected into a free running diabatic trajectory model and carried forward in time from December 1 to March 15. Vortex ozone loss was then estimated by comparing the ozone values of those parcels initiated early in the campaign with those parcels injected later in the campaign. Despite the variety of observational techniques used during SOLVE, the measurements provide a fairly consistent picture. Over the whole vortex, the largest ozone loss occurs between 550 and 400 K potential temperatures (~23-16 km) with over 1.5 ppmv lost by March 15, the end of the SOLVE mission period. An ozone loss rate of 0.04-0.05 ppmv/day was computed for March 15. Ozonesondes launched after March 15 suggest that an

additional 0.5 ppmv or more ozone was lost between March 15 and April 1. Finally, we find no evidence for a high mid-January loss as was reported for 1992 using the Match technique.

1. Introduction

One of the challenges in assessing polar winter chemical ozone loss is untangling the effects of dynamics and chemistry. Dynamical descent of vortex air during the fall and winter will cause lower stratospheric ozone to increase. In contrast, heterogeneous chemical processing of vortex air will decrease ozone. In addition, air from mid latitudes will occasionally intrude into the vortex. Since stratospheric, mid-latitude air below ~23 km has generally a lower ozone concentration than the vortex interior in mid-winter, the in-mixing of midlatitude air, like chemistry can also decrease ozone amounts within the vortex.

One approach to untangling dynamical and chemical processes in estimating ozone loss is to use simultaneous conservative tracer measurements. For example, Schoeberl et al. [1991] used N_2O measurements to estimate Arctic ozone loss during the late winter Airborne Arctic Stratospheric Expedition (1989). The idea is to tag ozone with a conservative tracer value and compare ozone amounts with similar conservative tracer value during the chemical loss period. The ozone-conservative tracer correlation shifts in the presence of chemical loss, and this can be used to remove the meteorological effects. Pseudo tracers have also been used separate chemistry from dynamics in estimating ozone loss. For example, Manney et al., [1994] and Grant et al. [2001] use potential vorticity (PV) as a pseudo tracer to estimate ozone loss from MLS data, but this technique is requires high quality PV computations and PV is not strictly conserved under diabatic processes. Sinnhuber et al. [2000] use a passive ozone tracer in their chemical transport model and estimate ozone loss by comparing ozone observations with the passive tracer.

Plumb et al. [2000] has pointed out that conservative tracer-ozone correlations should not be used over extended periods because when continuous mixing into the vortex interior occurs the tracer relationships are altered even if there is no chemistry. This can lead to incorrect estimations of vortex ozone loss and denitrification. To avoid this problem, Richard et al. [2001] has computed the ozone loss during the SOLVE (Sage III Ozone Loss and Validation Experiment) 1999-2000 winter period using ozone and two conservative tracers.

Unfortunately most ozone measurements are made without the simultaneous measurement of long-lived tracer fields (e.g. lidar ozone measurements, some satellite measurements, and ozonesondes). Thus we need to be able to estimate ozone loss without the use of long lived tracers. In this paper, we use two techniques to estimate ozone loss during the SOLVE campaign (December 1999-March 2000). The first technique is to use a simple regression analysis of ozonesondes and Polar Ozone and Aerosol Measurement III (POAM) data (reference). This analysis can be performed for two reasons. First, the SOLVE campaign was coordinated with the Third European Stratospheric Experiment on Ozone (THESEO) campaign so there were a significant number of ozonesondes launched within the polar vortex from November 1999 to April 2000. Meteorological analysis show that the vortex was cold and persistent with no major stratospheric warmings in the lower stratosphere [Manney and Sabutis, 2000]. Second, back trajectory calculations we have performed from March 15 to December 20 also show that there were no significant intrusions of middle latitude air into the vortex during the winter period. Because of this fortuitous isolation, a simple regression analysis of the ozone data should provide a reasonable assessment of the average vortex ozone loss over the winter period.

The second technique we use to analyze the SOLVE ozone data employs a diabatic trajectory model. In order to compute the ozone, trajectories are initiated whenever a measurement is made. By comparing vortex air parcels initiated early in the integration period with measurements late in the period, ozone loss can be estimated. This new technique does not depend on any assumption about the accuracy of any individual parcel trajectory only that statistics of the air parcels not be biased. This approach is unlike the Match technique [van der Gathen et al., 1995; Rex et al, 1997, 1998, 1999] which does depend on the accuracy of trajectory air mass predictions.

2. Procedure

Measurements of stratospheric ozone from five instruments were used in this study. The instruments are briefly described in this section, and their measurement parameters, such as vertical resolution and measurement error, are also given (see also Table 1).

Electrochemical Concentration Cell (ECC) ozonesondes are launched periodically on balloons and reach altitudes of up to 35 km [Komhyr et al., 1995]. They measure ozone by pumping air through potassium iodide (KI) solutions of different concentrations, contained in separate cathode and anode chambers. The solutions are buffered with potassium bromide. The presence of ozone causes I_2 to be formed, which is then converted to I^-, giving rise to an electrical current. ECC ozonesondes have been used in a number of intercomparison campaigns [Komhyr et al., 1995, Steinbrecht et al., 1999], giving a good indication of their measurement precision and accuracy as shown in Table 1 [Komhyr et al., 1995].

POAM III [Lucke et al., 1999] is a nine-channel (0.354 to 1.018 mm) solar occultation instrument designed to measure stratospheric profiles of ozone, NO_2 and water vapor densities, aerosol extinction at five wavelengths, and temperature. It was launched on the French Satellite Pour Observation de la Terre (SPOT) 4 satellite on March 23, 1998, into a sun-synchronous orbit at an altitude of 833 km, an inclination of 98.7°, and a period of 101.5 min; the descending node is crossed at 10:30 LT. As seen from the satellite, the Sun rises in the north polar region and sets in the south polar region 14.2 times per day.

The latitude of the POAM measurements varies slowly throughout the year between 55°N and 73°N and between 63°S and 88°S, with essentially identical coverage from year to year. All measurements in the northern hemisphere (NH) are made at satellite sunrise, and all measurements in the southern hemisphere (SH) are made at satellite sunset. This corresponds to local sunset in the NH throughout the year, to local sunrise in the SH during the Austral fall and winter, and to local sunset in the SH during the spring and summer.

The POAM Version 3 data algorithm validation has been performed using comparisons with HALOE version 19 (O_3, NO_2, H_2O and aerosol), SAGE II version 6.0 (O_3 and aerosols) and ozonesondes (O_3). For O_3, POAM generally agrees to within 5 to 8% with SAGE II, HALOE and ECC ozonesondes in the altitude range from 15 to 60 km. Somewhat larger disagreements (10 -15%) are seen below 15 km.

The NASA Langley airborne UV Differential Absorption Lidar (DIAL) system has been used to measure ozone, aerosol, and cloud profiles during four previous stratospheric ozone investigations, affording the opportunity for many comparisons with other ozone measuring instruments [Browell, 1989; Margitan et al., 1989; Browell et al., 1990, 1993, 1998; Grant et al., 1998]. This system uses two frequency-doubled Nd:YAG lasers to pump two high-conversion-efficiency, frequency-doubled, tunable dye lasers. In stratospheric O_3 investigations, the two

frequency-doubled dye lasers are operated independently with one tuned to 301 nm for the O_3 DIAL on-line wavelength and the other tuned to 311 nm for the off-line wavelength. All of the beams are transmitted in the zenith direction through a 40-cm-diameter fused silica window. The atmospheric backscattered laser returns are collected by a 36-cm telescope, optically separated, and directed on to different detectors.

The UV Photometer used for in situ O_3 measurements on the ER-2 is based on the design of Proffitt and McLaughlin [1983]. It uses a mercury lamp emitting radiation centered at 254 nm. Since it employs two absorption chambers, it can make measurements with a 1-s time constant.

The NASA GSFC/LaRC Airborne Raman Ozone, Aerosol and Temperature Lidar was flown for the first time during the SOLVE mission. A detailed description of the instrument and all the measurements is currently in preparation for publication [McGee et al., 2001]. The ozone measurement is made using the differential absorption technique: a XeCl excimer laser (200 mJ at 200 Hz) transmits 308 nm radiation, which is absorbed by ozone; and 355 nm from a Nd-YAG laser is used as the atmospheric reference. The beams are transmitted co-axially with the 16" receiver telescope, and the return signals are separated using dichroic beamsplitters and interference filters. All signals are photon counted. In order to ensure linearity over a dynamic range greater than 10^6, up to five separate detectors are used for each wavelength. The precision of the ozone measurement, as well as the vertical resolution, is variable depending on the altitude. The figures in Table 1 are generally representative for nighttime measurements. During daytime (solar zenith angles ~ 75 degrees), the upper altitude is generally limited to 26 km.

2.1 Vortex ozone regression analysis

For the POAM and ozonesonde time series regression analysis, we interpolate the ozone measurements onto vortex interior surfaces that are diabatically descending in time. The descent rates are determined from the ensemble average descent of parcels using the trajectory calculation discussed below. The data are first processed by selecting only observations within the vortex edge at 520 K as determined by the the isentropic MPV gradient [Nash et al., 1996] (here after Nash algorithm). Figure 1 shows the ozonesonde and POAM equivalent latitude locations at 520 K relative to the vortex edge at 520K. (For the definition of equivalent latitude, see Butchart and Remsburg [1986]), No adjustment is made in these calculations for the drift of the ozonesonde balloon.

Figure 2a shows the ozonesonde data time series for those measurements within the vortex edge. The appearance of bands of high modified potential vorticity (MPV) [Lait, 1994] and ozone at upper levels demonstrates that even though the ozonesonde or POAM measurement can be within the vortex at 520K the measurement can outside of the vortex at higher altitudes due to the tilt of the vortex or the motion of the balloon. At these higher altitudes, the ozone mixing ratio outside the vortex is higher than inside the vortex. To reduce the amount of non-vortex observations, a second filter is applied to the data. First, the data are fit to a second order polynomial along the descending PT surfaces shown (descending lines). If the observations deviate by more than 1 ppmv from the fit, that data point is removed. The result is shown in Figure 2b and indicates that this method does a reasonable job of eliminating additional outlying observations while still retaining the essential character of the time series. After application of the second filter, the data are then refit to the descending surfaces shown in Figure 2. Both POAM and ozonesonde data are processed in the same way, the POAM data are not shown.

2.2 Trajectory Analysis

In the trajectory method, we simply inject parcels when ozone measurements are made and continue to move the parcels diabatically until the end of the integration period. Of course, some of the parcel integrations will be up to 105 days long so we only expect that the distribution of the parcels will be accurate in a statistical sense. In other words, the loss amounts calculated using this technique should approximate the vortex average. We have tested the fidelity of this approximation by comparing the March 15, 2000 difference between the temperature obtained by averaging the parcels within the vortex and the analyzed average vortex temperature. For the isentropic levels between 400 – 600K, the temperature difference is less than a degree except at 400K where it is 4.5K. This means that the using parcel averages reasonably approximates the vortex average except at 400K. At 400K, the vortex is fairly broken up and the vortex average is hard to define.

By comparing ozone amounts associated with different vortex parcels initiated at different times we can estimate the net loss ozone loss. The population of parcels examined at the end of the integration is different data set from ozonesonde and POAM regression analyses. For example, measurements made at the edge of the vortex are included in the simple regression analysis, but those measurements will probably not be included in the trajectory analysis since the vortex edge material erodes away during the winter. In other words, many edge measurements, represented as parcels, will end up in middle latitudes and thus not be included in the final analysis.

The trajectory integration begins on December 1, 1999 and is carried through to the March 15, 2000. POAM and ozonesonde measurements were made over the whole winter period. The December period corresponds to the first SOLVE aircraft segment during which only DC-8 lidar and in situ ozone measurements were made. The DC-8 in situ measurements are below the region of interest and not used in this analysis. During the January and March segments of SOLVE, ER-2 in situ ozone measurements are added to the DC-8 measurements.

The diabatic trajectory descent method has been generally validated using HALOE methane observations within the austral and boreal polar vortices [Rosenfield and Schoeberl, 2001]. We have also compared the descent of the long-lived tracer SF_6 during SOLVE with trajectory estimates. Best agreement between the vortex interior changes on SF_6 between January and March was obtained when the net diabatic net heating was not globally balanced and linear interpolation of the heating rates between mandatory pressure levels was used. Usually spline interpolations are used in projecting the diabatic heating rates onto the parcel locations. However, when heating rates become very small, the spline methods can create unrealistic local minima.

Observations injected into the trajectory model were screened to remove any obviously bad measurements, and any data taken below the 330K potential temperature (PT) surface were ignored. For ozonesonde data, either the wind observations recorded with the ozonesonde or global meteorological analyses were used to compute the drift of the balloon with altitude. UV Differential Absorption Lidar (DIAL) [Browell et al., 1998] and Airborne Ozone and Temperature Lidar (AROTEL) data [McGee et al., 2001] data were interpolated from the aircraft geometric coordinates to PT surfaces using the United Kingdom Meteorological Office (UKMO) global analysis [Swinbank and O'Neill, 1994]. The in situ pressure and temperature data from the ER-2 data were used to compute the potential temperature of the ozone data from that platform.

The large amount of lidar data creates a problem with this analysis approach since a single flight of the DC-8 with the two ozone lidars creates more observational data than the entire winter set of ozonesondes. However, most of the lidar data has a high degree of horizontal correlation and thus the extra observations do not significantly add information on the large-scale ozone changes. Thus we have thinned the lidar and ER-2 data sets using the distance that the autocorrelation falls to zero to provide an "equivalent ozonesonde" data set. Within the vortex, the autocorrelation distance is about 400 km for DIAL, 250 km for the in situ ozone measurements from the ER-2 and 300 km for AROTEL although these numbers vary a little from flight to flight. These different autocorrelations arise from different post processing algorithms that include averaging of the data to increase the precision.

After integrating the trajectory model forward from Dec 1, 1999 to March 15 2000, over 200,000 observations have been inserted. Both measurements outside and inside the vortex are included in this analysis. Figure 3 shows the altitude and equivalent latitude distribution of the parcels on March 15. It is apparent from the figure that many of the parcels have been shed from the vortex as might be expected from ongoing vortex erosion.

As mentioned above, ozone loss is computed by comparing the ozone concentration of parcels generated throughout the integration period. This Lagrangian approach to assessing ozone loss is very different from the Match technique [van der Gathen et al., 1995, Rex et al., 1999]. The Match technique calculates the difference between successive ozone measurements (usually ozonesondes) that are connected using a trajectory calculation. Thus, the Match requires frequent ozonesonde launches, and an accurate forecast of the motion of the measured air mass. The technique described here does not rely on the accuracy of individual trajectories but on the accuracy of the ensemble that, from our test described above, appears to accurately represent vortex conditions.

3 Results

3.1 Regression analysis of ozonesonde and POAM data

The ozone change using the regression analysis from December 1, 1999 to March 15, 2000 is shown in Figure 4. As mentioned above, the data are fit to each descending surface shown in the figure. By mapping the data fits to the descending surfaces , and assuming isolation of the vortex from midlatitudes, the loss shown in Figure 4 should entirely be a result of chemical processes. The standard deviation of the data fit is shown in Figure 8 which will be discussed later.

The ozonesonde and POAM data generally agree: the ozone change (loss) is largest in March, and the rate of this change is also largest during the February-March period. By March 15 vortex averaged loss amounts are greater than 2 ppmv (between 55%-65%). This loss decreases rapidly with altitude above 530K. Prior to the main decrease period in February-March, the POAM series indicates some loss above 480K during January. Below we discuss the March and January periods. The ozonesonde increase in ozone seen in the Fig. 4a during the December period will be discussed in the summary section.

3.1.1 January ozone loss

Figure 5 shows the UKMO analyzed temperatures of the vortex during the SOLVE period. The most intense cold periods occurred in late December and January and at altitudes coincident with POAM ozone loss in January. Formation of PSCs in this period would enhance reactive chlorine levels, and thus it is plausible that there is some ozone loss occurring in January. Given our

understanding of the photochemistry of polar ozone loss [Solomon, 1999], loss at this time would have to take place near the edge of the polar vortex where the solar illumination is the greatest. Midwinter ozone loss near the edge of the vortex has recently been derived for the Antarctic [Lee et al., 2000].

To further investigate the possibility of edge loss, we have calculated the fraction of sunlight observed by air parcels at the 520K potential temperature surface using trajectory calculations. The probability distribution functions (PDF) for equivalent latitude and solar exposure these data are shown in Figure 6.

Solar exposure was computed by performing a seven day reverse domain fill back trajectory calculation for each day of the SOLVE winter period (see Schoeberl and Newman, 1996), and then computing the amount of time each parcel encountered to solar zenith angles less than 90°. The solar exposure map generated at 1° by 1° resolution is used to estimate the parcel solar exposure shown in Figure 6. Given our current understanding of the polar ozone loss processes and the observation of wide spread polar stratospheric cloud observations during December, solar exposure above zero means that some ozone loss should take place for those air parcels. The mobility of the Arctic vortex allows even high equivalent latitude parcels to have some exposure. Although the mean solar exposure for ozonesonde and POAM parcels is nearly the same, the POAM distribution is more skewed toward higher solar exposures (Fig. 6b) while the ozonesonde PDF shown in Fig. 6a is skewed in the other direction. This is not very surprising since POAM requires sunlight to make measurements, and during January 2000 the POAM measurements tended to be at lower equivalent latitudes near the edge of the vortex (as seen in Fig. 1b). Since solar exposure will not be a linear indicator of ozone loss, the skew of the distribution is a more important factor than the mean. To check the sensitivity of the diagnosed ozone loss to solar exposure, we performed a series of experiments restricting the POAM measurements to higher equivalent latitudes in the period December 1- Feb. 15. The resultant PDF for >75° restriction is shown in Figure 6c. The restriction in equivalent latitude has the effect of also reducing the solar exposure as would expected from the arguments above.

Figure 7 summarizes the results of several experiments in which the equivalent latitude of solar exposure were restricted. The conclusion drawn from these experiments is that when the population of the POAM data is altered so that solar exposure is reduced, the data sets tend to show very little ozone loss. The ozonesonde data shows a different effect, since the population is restricted to higher equivalent latitudes, the January increase in ozone seen in Fig. 4a is reduced. Because the ozonesonde data set is already has very low solar exposure, restricting the data set to high equivalent latitudes does not significantly alter the solar exposure of the population, but it does reduce the population of points near the edge of the vortex. This eliminates the occasional edge point that has high ozone (see Fig. 2). This result shows that the increase in ozone seen in the ozonesonde analysis (Fig. 4a) is probably due to inclusion of edge points, not the result of any real increase.

We conclude from this analysis that ozone loss by mid January is small and restricted to lower equivalent latitudes or parcels with larger solar exposure. We also conclude that the POAM and ozonesonde data are telling the same story when the population of measurements are restricted to equivalent conditions. This conclusion is supported by the model calculations made during SOLVE (Reprobus model group, private communication, 2000) that also show that January ozone loss is confined to the illuminated edge of the vortex.

3.1.2 March ozone loss

Figure 8 compares the March 15 loss amounts between the POAM and ozonesonde series. The trajectory analysis is also shown, and will be discussed below. Column ozone change is also indicated in the caption. Generally there is good agreement between the data sets below 460 K. At higher altitudes the ozonesonde and POAM data sets show an offset of about 0.5 ppmv or more. The discrepancy arises from the trends in early winter where the ozonesonde data show increases in ozone while the POAM analysis shows a decrease (Fig. 4). By March 15, the ozone loss rates (Fig. 9) agree reasonably well with a rate of ~0.04 ppmv/day. This is nearly the same rate as is seen during peak Antarctic ozone loss rate period [Wu and Dessler, 2001] and is what might be expected in a fully sunlit vortex which contains high levels of ClO as was observed during SOLVE [Santee, et al., 2000].

As noted above the 0.5 ppmv discrepancy between POAM and ozonesonde data in Figure 8 also arises from the sampling bias. High ozonesonde measurements amounts in mid-January (Fig 2b) push the January ozonesonde amounts above the POAM amounts. The second order fit to the ozonesonde data becomes more parabolic with a peak in early-January. As a result, the December 1 ozonesonde fit value is below the POAM fit value thus giving a smaller net ozone loss for the ozonesonde data. This effect also gives rise to the increase in ozone seen in Fig. 4a. If the ozonesonde data sets are filtered to high equivalent latitudes, the January peak is reduced and the ozonesonde and POAM data are in closer agreement (Fig. 7).

3.2 Trajectory analysis

As discussed in Section 2.2 we use the trajectory model to compare all ozone measurements within the vortex. Figures 10a,b show the analysis for March 15 at two isentropic surfaces, 460K and 520K. Separate analyses are performed for isentropic levels 20 K apart from 400-600 K. The data are selected for analysis by marking parcels within a ±2K window of the target potential temperature within the vortex edge (see Fig. 10). Usually the vortex edge from the Nash algorithm is used; however, visible in Figure 10 is a lobe of the main vortex which, on March 15, has separated from main vortex toward the upper right of the figure. This lobe may contain midlatitudes air that has mixed in during the process of separation. The Nash algorithm, at some potential temperature surfaces, will place the edge around that lobe, so a higher PV edge value is used in those cases. Once parcels have been selected, a second order fit to the data versus parcel is performed. A cursory examination of the data reveals that some ozone observations are quite far from the ensemble mean with the same age. These observations usually originate near the edge of the vortex where the chemical boundary and the MPV boundary do not exactly line up. To reduce the influence of these points, the data are filtered so that points 0.5 ppmv from the regression curve are rejected. Although this sounds like a severe rejection criterion only about 15% additional data are rejected using this criteria compared to a rejection criteria of 2 ppmv.

Figure 10 shows the mix of the data used. Generally, ozonesonde, AROTEL, and POAM data contribute at all altitudes. Dial makes a large contribution to the data below 500K. Compared to the other data sets, the ER-2 makes a negligible contribution. Because of the variable number of parcels that exist with any given age, the regression analysis is performed by computing the daily averaged ozone as a function of age. The daily average is shown in Figure 10 (upper right) as small crosses (see caption for Fig. 10)

Figures 8 and 9 compare the trajectory computed Dec. 1 - March 15 loss amounts and March 15 loss rates with the ozonesonde and POAM regression analyses. Trajectory results are labeled BFT for Brute Force Trajectory. In general, there is good agreement between the three techniques. The trajectory analysis shows a somewhat lower loss amount in the main loss regions (below 520K) than POAM, but produces about the same loss rate as the POAM and ozonesonde analysis.

The difference in the loss amounts can probably be attributed to the sample population. In the trajectory scheme the number of parcels used in the analysis are those remaining within the vortex on March 15. In the ozonesonde and POAM analysis the population of points includes any measurements inside the vortex when the measurement is made. It is more likely that a parcel initiated deep within the vortex will still be within the vortex by March 15. Thus the trajectory technique will not consider many of the POAM observations at the edge of the vortex since these will have been eroded to middle latitudes.

4 Discussion and summary

The SOLVE winter period (December 1, 1999 – March 15, 200) was characterized by cold temperatures, a fairly isolated Arctic stratospheric vortex and significant ozone loss. In this paper we have performed analyses using two methods: a simple regression analysis of ozonesonde time series and the POAM satellite time series within the vortex and a trajectory analysis which includes both of those data sets as well as DC-8 lidar and ER-2 in situ ozone data. The trajectory analysis is a new approach where measurements are continuously injected into the free running trajectory calculation. At the end of the trajectory integration, all parcels within the vortex are compared. The plot of ozone measurement amount versus age of the parcels shows the ozone change.

By mid-January the POAM regression analysis reveals a small ozone loss that is not apparent from the ozonesonde analysis. The disagreement between the two data sets can be minimized by reselecting the observations to reduce the solar exposure and the number of vortex edge measurements. Thus, the likely source of the disagreement between POAM and ozonesonde analysis is (1) ozone loss at the edge of the vortex for parcels that have been exposed to sunlight and (2) the occasional high ozone value from an ozonesonde which is not completely inside the vortex. The fact that ozone loss may take place first at the edge of the vortex has already been shown from Antarctic observations [Lee et al., 2000]. Thus, given a fairly symmetric nearly pole centered vortex, as occurred during SOLVE, the development of edge loss is not a surprise. Model calculations (see this issue) show that January loss is higher at the edge of the vortex than in the interior. Because the POAM instrument samples preferentially along the vortex edge in January 2000, the population of POAM measurement emphasizes edge ozone loss. The important point here is that ozone loss within the vortex in January during SOLVE was apparently non-uniform. Because of the non-uniform ozone loss the January, the vortex cannot be characterized as a single entity with regard to ozone loss. Furthermore, the edge is a barrier to mixing [Schoeberl et al., 1989; Bowman 1993, 1996] so ozone loss near the vortex edge would be very slowly communicated to the interior.

Our analysis does not show the high ozone loss rates of 0.05 ppmv/day in mid-January as deduced by the Match analysis for the 1992 winter period [Rex et al., 1998]. In fact, the Match computed January ozone loss rate approached the loss rate we compute for the fully activated, sunlit mid-March polar vortex. Becker et al. [1998] could find no chemical explanation for the high Match loss rates. It is possible that the losses estimated by the Match technique were occurring mostly in regions of the vortex where the solar exposure was high.

By the middle of March our analysis shows ozone loss amounts between 1.5-2 ppmv (45-55%, respectively) for the winter period (Fig. 8). POAM regression analyses show the higher ozone loss (2 ppmv), compared to the ozonesonde regression analyses and the trajectory calculation. This disagreement is small given the small number of ozonesonde measurements compared to POAM. The data analysis is sensitive to the selection of points near the edge of the vortex. These data points are eroded away from the vortex during the winter. To show this sensitivity,

we have selected only POAM parcels from the trajectory analysis and performed a 2nd order regression analysis on the data subset. These are POAM initiated parcels that are still within the vortex by March 15. Figure 11 shows that if only the POAM parcels remaining within the vortex are used then the ozone loss is 0.75 ppmv less than computed using the POAM regression analysis. Figure 12 shows the PDF of the Jan 1-20 equivalent latitudes for the POAM points used in the trajectory analysis. Figure 12 should be compared to Figure 6b. In Figure 6b the mean equivalent latitude for the POAM regression analysis is ~70° where the mean equivalent latitude for the trajectory POAM points over the same period is ~80°. The means that the POAM points used for the trajectory analysis (those remaining in the vortex at March 15) were those with almost no solar exposure (compare Figures 6b and 6c to see the impact of restricting equivalent latitude has on solar exposure) and thus show very little ozone loss during this period.

A number of other estimates of ozone loss within the December 1999 - January 2000 polar vortex have been made. Santee et al. [2000] computed ozone loss from late winter (February – mid March) from the Microwave Limb Sounder (MLS) observations. They estimated a February vortex averaged 465K loss rate of 0.04±0.01 ppmv/day. This loss rate is comparable to our March 15 loss rate, but on the high side for February. From both ozonesonde and trajectory analysis we compute a mid-February 465K vortex loss rate of ~0.025 ppmv/day. Figure 13 shows the loss rate computed from the ozonesonde analysis. In mid February, the loss rate maximizes near 500K, and given the vertical weighting functions of the MLS data, their ozone loss rate is probably correct to within their error bars.

Richard et al. [2001], using ER-2 aircraft data, have also computed a loss rate between the beginning of January and the end of February and for the period from the end of February to mid-March. In agreement with our analysis they concluded that the January loss rates were small but by mid March the loss rate was 0.05 ppmv/day. This is in good agreement with our calculations as well (Fig. 9, 13). Assuming the high loss rates, and applying them to a 38-day period Richard et al. obtain a loss amount of 2 ppmv. Our calculations suggest that this is an over estimate since the loss rates are increasing rapidly over this period, and it is probably inappropriate to apply the highest loss rate to the last 38 days. However, in broad scope, the two computations are in agreement in both the loss rate and amount of loss.

Ozonesondes continued to be launched into vortex after March 15, and the ozonesonde regression analysis shown in Fig. 4a extends to the end of March. By that time, nearly 70% of the ozone was lost (more than 2 ppmv) even though the vortex rapidly shrank in area during that period. Sinnhuber et al. [2000] also show loss rates of 70% by the beginning of April using the Ny-Alesund ozonesondes. Their loss amounts are nearly 2.5 ppmv compared with ours which are just over 2.0 ppmv for the same period. The differences can be traced to our selection of the data within the vortex MPV edge. Some of the late March Ny-Alesund ozonesondes are outside the MPV edge as determined by the gradient, and are not included in our analysis. This is a period when the vortex is eroding rapidly and large fragments have broken off the main vortex. If we restrict our analysis to just Ny-Alesund observations and relax the edge criterion for March we obtain the Sinnhuber et al. values. However, it is not clear that the Sinnhuber et al. number represents a vortex average loss amount or an upper limit on the loss. DIAL measurements within the vortex interior on March 13, 2000 show a 1 ppmv range at 18 km over large regions. Thus it is not surprising that the various analysis techniques arrive at ozone loss numbers which differ to within 0.5 ppmv.

We have also done a computation of the column ozone lost from December 1999 through March 15, 2000. This loss can be that can be compared with that estimated from the Total Ozone Mapping Spectrometer (TOMS). Taking the 63° –90°N average of all the TOMS March data up

to 1990 and comparing that with the average in March 2000, we find that polar total ozone decreased by ~61 Dobson Units (DU). The year-to-year variability prior to 1990 was about 26 DU peak to peak so this decrease is well beyond the pre-1990 data range. In 1986, the March polar average temperatures were close to that observed during SOLVE and the March mean column ozone was 430 DU. The average for SOLVE March period was 385 DU thus at least 45 DU could be plausibly assigned to chemistry, assuming, as a lower bound, that none of the loss in 1986 was chemical. From Figure 8, the chemical decrease is computed to be between 44 (ozonesonde) to 57 DU (POAM) which is in reasonable agreement with this crude estimate.

Acknowledgements

The authors wish to acknowledge the SOLVE and THESEO management, logistics personnel, and the staff at Arena Arctica,, Kiruna, Sweden for excellent mission support. We would also like to thank the DC-8 and ER-2 aircraft managers, ground crew, and pilots for their superior performance during the SOLVE misssion. This work was funded by NASA's Upper Atmosphere Research Program and the Earth Observing System Program Office.

References

Becker, G, R. Muller, D. McKenna, M. Rex, and K. Carslaw, Ozone loss rates in the Arctic stratosphere in the winter 1991/92: Model calculations compared with Match results, Geophys. Res. Lett., 25, 4325,-4328, 1998.

Bowman, K. P. Large scale isentropic mixing properties of the Antarctic polar vortex from analyzed winds, J. Geophys. Res., 98, 23013-23027, 1993

Bowman, K. P. Rossby wave phase speeds and mixing barriers in the stratosphere, Part 1: Observations, J. Atmos. Sci., 53, 905-916, 1996

Browell, E. V., S. Ismail, and W. B. Grant, Differential absorption lidar (DIAL) measurements from air and space, Appl. Phys. B67, 299-410, 1998.

Browell, E. V., Differential absorption lidar sensing of ozone, Proc. IEEE, 77, 419-432, 1989.

Browell, E. V., et al., Airborne lidar observations in the wintertime Arctic stratosphere: Ozone, Geophys. Res. Lett., 17, 325-328, 1990.

Browell, E. V., C. F. Butler, M. A. Fenn, W. B. Grant, S. Ismail, M. Schoeberl, O. B. Toon, M. Loewenstein, and J. R. Podolske, Ozone and aerosol changes observed during the 1992 Airborne Arctic Stratospheric Expedition, Science, 261, 1155-1158, 1993.

Butchart, N. and E. Remsberg, The area of the stratospheric polar vortex as a diagnostic for tracer transport on an isentropic surface, J. Atmos. Sci., 41, 1319-1339, 1986.

Grant,W. B., E. V. Browell, C. Butler, and S. Kooi, Use of potential vorticity as a conserved tracer to estimate Arctic polar vortex ozone loss during the winter of 1999/2000, J. Geophys. Res., (this issue), 2001.

Grant, W. B., M. A. Fenn, E. V. Browell, T. J. McGee, U. N. Singh, M. R. Gross, I. S. McDermid, L. Froidevaux, and P.-H. Wang, Correlative stratospheric ozone measurements with the airborne UV DIAL system during TOTE/VOTE, Geophys. Res. Lett., 25, 623-626, 1998.

Komhyr, W. D., R. A. Barnes, G. B. Brothers, J. A. Lathrop, and D. P. Opperman, Electrochemical concentration cell ozonesonde performance evaluation during STOIC 1989, J. Geophys. Res., 100, 9231-9244, 1995.

Lait, L. R., An alternative form for potential vorticity, J. Atmos. Sci., 51, 1754-1759, 1994.

Lee, A. M., H. K. Roscoe, and S. Oltmans, Model and measurements show Antarctic ozone loss follows edge of polar night, Geophys. Res. Lett, 27, 3845-3848, 2000.

Lucke, R. L., et al., The Polar Ozone and Aerosol Measurement (POAM) III instrument and early validation results, J. Geophys. Res., 104, 18,785-18,799, 1999.

Lumpe, J. D., R. M. Bevilacqua, K. W. Hoppel, S. S. Krigman, C. Brogniez, E. P. Shettle and D. Kriebel, POAM II retrieval algorithm and error analysis, J. Geophys. Res., 102, 23,593-23,614, 1997.

Manney, G. L., et al. , Chemical depletion of ozone in the Arctic lower stratosphere during winter 1992-93, Nature, 370, 429-434, 1994.

Manney, G. L. and J. Sabutis, Development of the polar vortex in the 1999-2000 Arctic winter stratosphere, Geophys. Res. Lett., 27, 2589-2592, 2000.

Margitan, J., et al., Intercomparison of ozone measurements over Antarctica, J. Geophys. Res., 94, 16,557-16,569, 1989.

McGee, T. J., et al., The AROTEL Instrument - an airborne lidar for stratospheric ozone, temperature and aerosols, Applied Optics, (submitted), 2001.

Nash, E. R., P. A. Newman, J. E. Rosenfield and M. R. Schoeberl, An objective determination of the polar vortex using Ertel's potential vorticity, J. Geophys. Res., 101, 9471-9478, 1996.

Plumb, R. A., D. W. Waugh and M. P. Chipperfield, The effects of mixing on tracer relationships in the polar vortices, J. Geophys. Res., 105, 10047-10062, 2000.

Proffitt, M. H., and R. J. McLaughlin, Fast-response dual-beam UV-absorption photometer suitable for use on stratospheric balloons, Rev. Sci. Instrum. 54, 1719-1728, 1983.
Rex, M., .et. al. Prolonged stratospheric ozone loss in the 1995-96 Arctic winter, Nature, 389, 835-838, 1997.

Rex., M. et al., In situ measurements of stratospheric ozone depletion rates in the Arctic winter 1991/92; a Lagrangian approach, J. Geophys. Res., 103, 5843-5853, 1998.

Rex., M. et al., Chemical ozone loss in the Arctic winter 1994/95 as determined by the MATCH technique, J. Atmos. Chem., 32, 35-59, 1999.

Richard, E. C., et al. Severe Chemical Ozone Loss Inside the Arctic Polar Vortex during Winter 1999-2000 Inferred from in-situ Measurements., (submitted to J. Geophys. Res.) 2001.

Rosenfeld, J. E., P. A. Newman and M. R. Schoeberl, Computations of diabatic descent in the stratospheric polar vortex, J. Geophys. Res., 99, 16,677-16,689, 1994.

Rosenfield, J. E and M. R. Schoeberl, On the origin of polar vortex air, submitted to J. Geophys Res., (submitted) 2001.

Santee, M. L., G. L. Manney, N. L. Livesey, and J. L. Waters, UARS Microwave Limb Sounder observations of denitrification and ozone loss in the 2000 Arctic late winter, Geophys. Res. Lett., 27, 3213-3216, 2000.

Schoeberl , M. R. and P. A. Newman, A Multiple Level Trajectory Analysis of Vortex Filaments,, *J. Geophys. Res.,* **100**, 25801-25815, 1996.

Schoeberl, M. R., M. H. Profitt, K. K. Kelly, L. R. Lait, P. A. Newman, J. E. Rosenfield, M. Loewenstein, J. R. Podolske, S. E. Strahan, and K. R. Chan, Stratospheric constituent trends from ER-2 profile data, J. Geophys. Res., 17, 469-472, 1990.

Schoeberl, M. R. et al., Reconstruction of the Constituent Distribution and Trends in the Antarctic Polar Vortex from ER-2 Flight Observations, *J. Geophys. Res.,* **94**, 16815-16845, 1989.

Sinnhuber et al., Large loss of total ozone during the Arctic winter of 1999/2000, Geophys. Res. Lett., 27, 3473-3476, 2000.

Solomon, S., Stratospheric ozone depletion: A review of concepts and history, Rev. Geophys. 37, 275-316, 1999.

Steinbrecht, W., R. Neuber, P. von der Gathen, P. Wahl, P., T. J. McGee, M. R. Gross, U. Klein, and J. Langer, Results of the 1998 Ny-Alesund Ozone Monitoring Intercomparison J. Geophys. Res., 104, 30,515-30,523, 1999.

Swinbank, R., and A. O'Neill, A stratosphere-troposphere data assimilation system, Mon. Wea. Rev., 122, 686-702, 1994

van der Gathen, P., et al., Observational evidence for chemical ozone depletion over the Arctic in winter 1991-92, Nature, 375, 131-134, 1995.

Wu, J. and A. E. Dessler, Comparisons between measurements and models of polar ozone loss, (submitted to J. Geophys. Res.), 2001.

Figure Captions

Figure 1.
The location of ozonesonde (part a) and POAM (part b) measurements used in the regression analysis with respect to equivalent latitude at 520 K. The vortex edge is shown as the dark line.

Figure 2.
Upper figure (part a) shows the ozonesonde data time series. Small arrows at the top show the ozonesonde times. Parallel descending lines (descent contours) show the change in potential temperature computed from descending parcel ensembles. Additional lines show modified potential vorticity (MPV) values. Lower figure (part b) shows the data after application of polynomial fit filter.

Figure 3.
The distribution of parcels from the trajectory calculation (white dots) as a function of the March 15 equivalent latitude and potential temperature plotted over the zonal mean temperature in Kelvin (colors and white contours). Parcels have been thinned by a factor of 10 (only 20818 shown). Vertical orange line shows the edge of the vortex computed using the Nash algorithm (see text).

Figure 4.
Ozone change starting from December 1, 1999 computed using ozonesonde observations (part a) and POAM observations (part b). Negative values indicate loss. Thin lines show the descent lines along which the analysis is performed.

Figure 5
Arctic vortex averaged and minimum temperatures during the winter 1999-2000. Temperatures cold enough for polar stratospheric cloud formation (~195K) occurred during most of the winter. The vortex average is the average of the temperature inside the vortex edge for each isentropic surface. Note that the coldest temperatures appeared to move to lower altitudes during the course of the winter.

Figure 6
The PDF for solar exposure and equivalent latitude for January 1-20, 2000. Part a, ozonesonde measurements; part b POAM measurements, part c POAM measurements restricted to > 75° equivalent latitude. Normalized solar exposure is defined as the fraction of the day the parcel encounters solar zenith angles less than 90°.

Figure 7.
A comparison of ozone loss between December 1, 1999 and January 15, 2000 using POAM and ozonesonde data versus potential temperature. The vortex average log pressure altitude times 7 km is shown on the left. The ozonesonde and POAM data have been filtered by equivalent latitude and solar exposure. The different filtering gives different loss amounts. The error bars show one standard deviation of the data from the regression analysis. Restricting the equivalent latitude has the same effect of reducing the solar exposure.

Figure 8.
Ozone change from the ozonesonde, POAM and trajectory time series. The error bars indicate the one standard deviation fit to the data time series. The column ozone change is computed for

the ozone profile change shown. Log pressure altitudes times 7 km are computed using the vortex average temperature for March 15. BFT indicates the trajectory estimate of ozone change.

Figure 9.
Same as Figure 8 except ozone loss rate from the ozonesonde, POAM and trajectory time series. The error bars indicate the one standard deviation fit to the data time series.

Figure 10.
Analysis of trajectory results for the 440K(part a) and the 520K (part b) surface. Upper left inset figure shows the selected points within the vortex at potential temperatures 440K ± 2K Upper right inset shows the parcels plotted as a function of measured ozone amount and time of initiation (age) before March 15. The data are averaged for each day and the averages are shown as crosses. The curve is the second order fit to the daily averaged data. The net ozone loss and peak loss rate are indicated in the figure. The data source key is shown in lower left inset which indicates the mix of data types (D= UV DIAL, P= POAM, H= HALOE, S= SAGE II, A= AROTEL,, E = ER-2 So = Ozonesonde, Avg. indicates the daily average of the data). Lower right inset shows the daily averaged initial potential temperature of the data versus the age. The second order fit (line) is used to compute the descent curves shown in Figure 2.

Figure 11.
Trajectory analysis of POAM data (BFT, dashed line)) compared with POAM regression series analysis of ozone change during the solve winter. Error bars are one standard deviation of the data from the fit.

Figure 12.
The distribution of equivalent latitudes for the POAM points used in the trajectory calculation from Jan 1-20. These are the points remaining within the vortex by March 15 when the trajectory calculation is terminated.

Figure 13
The ozone loss rate from the ozonesonde regression analysis (see Fig. 4a). The upper graph shows the computed rate along the descending potential temperature surfaces (dashed lines). The bottom graph shows the one standard deviation uncertainty for the surface marked in red in the upper figure.

Table 1. Ozone measurement parameters for the instruments considered in this work.

Instrument	Altitude Range	Resolution Vert. (km)	Resolution Horiz. (km)	Error (%)	References
AROTEL	14 km	0.5	70	2	McGee et al.[2001]
	20 km	2.0	70	12	
	25 km	1.0	70	5	
	30 km	3.0	70	25	
ECC					
Ozonesonde	to 16	0.3		<10	Komhyr et al. [1995] Steinbrecht et al. [1999]
	16-26			<5	
	26-31			10	
POAM	15-20	1.1-1.7	200	5-8	Lucke et al. [1999]
	20-50	1.1	200	5-8	
UV DIAL					
Nighttime	12-19	0.75	70	5-8	Browell et al. [1990, 1993,1998] Grant et al. [1998]
	19-25	0.75	140	<10	
Daytime	12-19	0.75	70	5-10	
	19-21	0.75	140	<10	
UV Photometer	0-22 km	0.01	0.01	3	Proffitt and McLaughlin [1983]

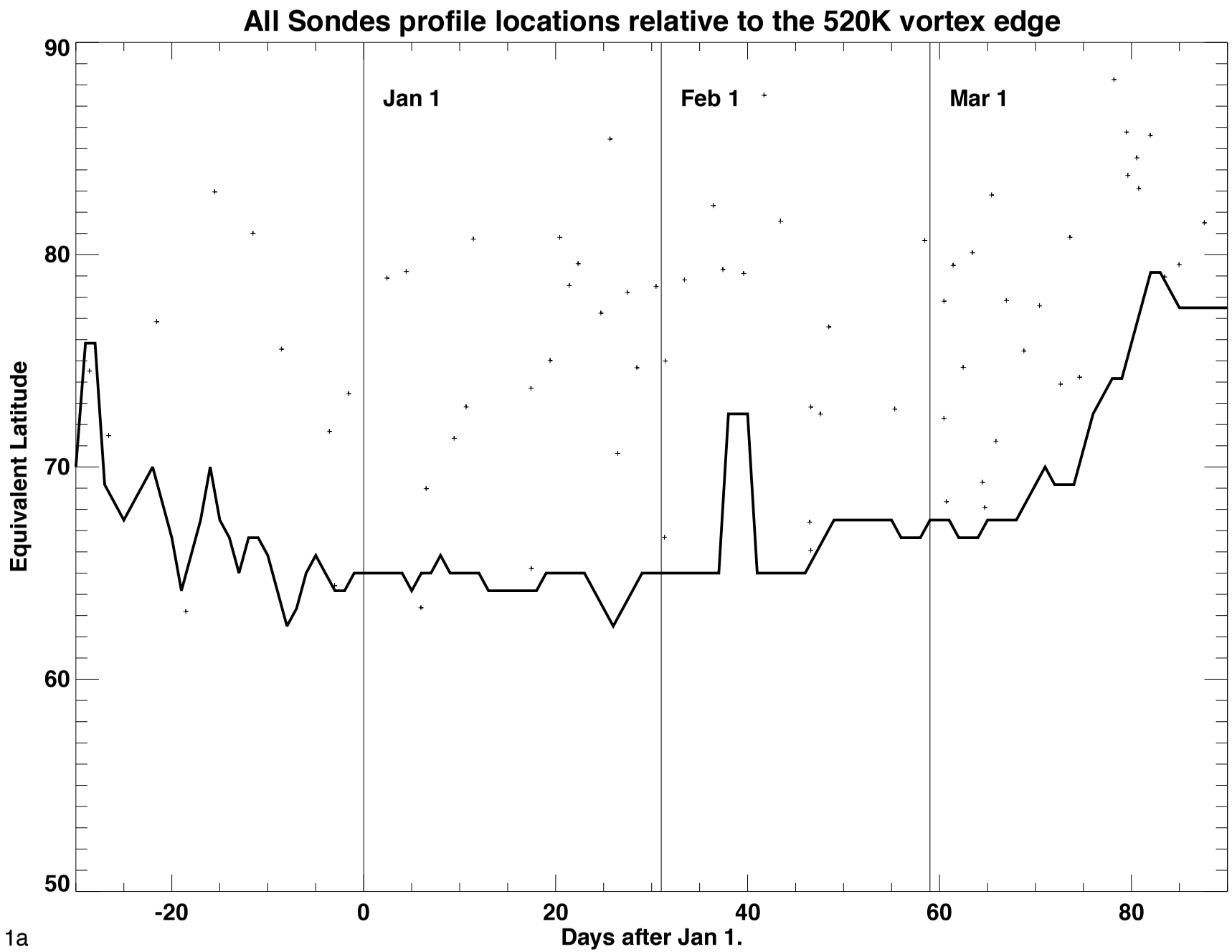
All Sondes profile locations relative to the 520K vortex edge
Jan 1
Feb 1
Mar 1
Equivalent Latitude
90
80
70
60
50
-20
0
20
40
60
80
Days after Jan 1.

Fig. 1a

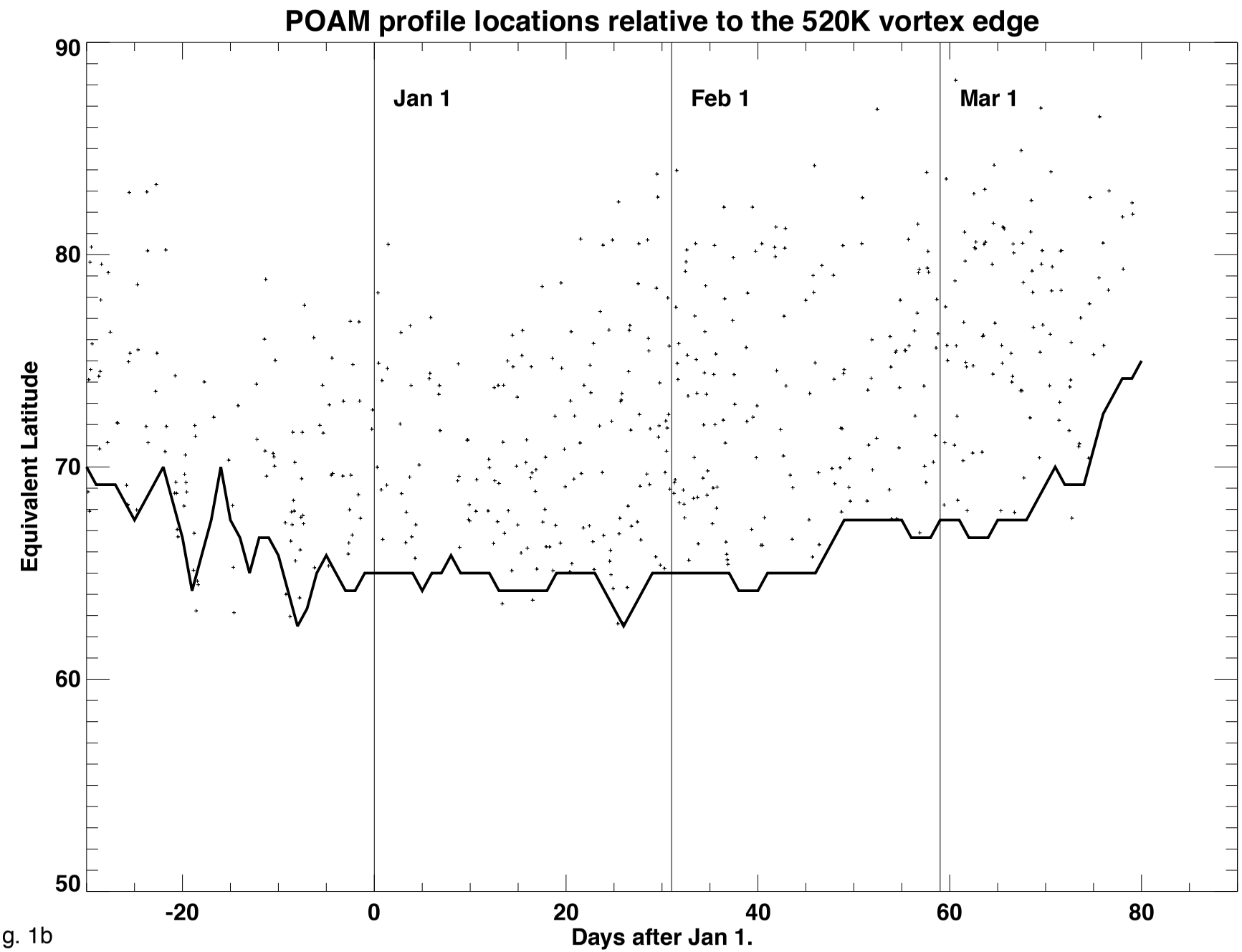
POAM profile locations relative to the 520K vortex edge
Jan 1
Feb 1
Mar 1
Equivalent Latitude
90
80
70
60
50
-20
0
20
40
60
80
Days after Jan 1.

Fig. 1b

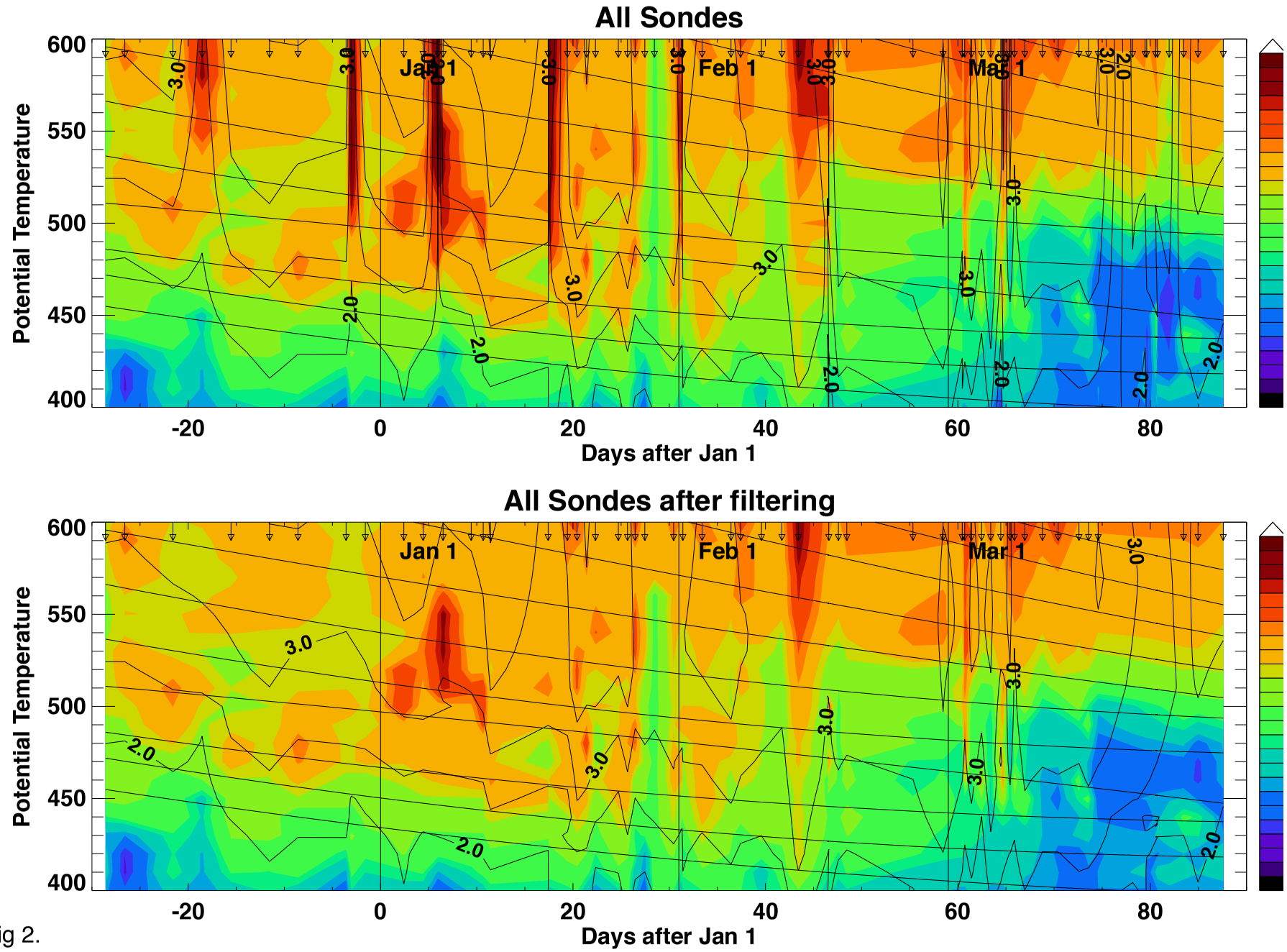
All Sondes
Jan 1
Feb 1
Mar 1
Potential Temperature
600
550
500
450
400
-20
0
20
40
60
80
Days after Jan 1
All Sondes after filtering
Jan 1
Feb 1
Mar 1
Potential Temperature
600
550
500
450
400
-20
0
20
40
60
80
Days after Jan 1

Fig 2.

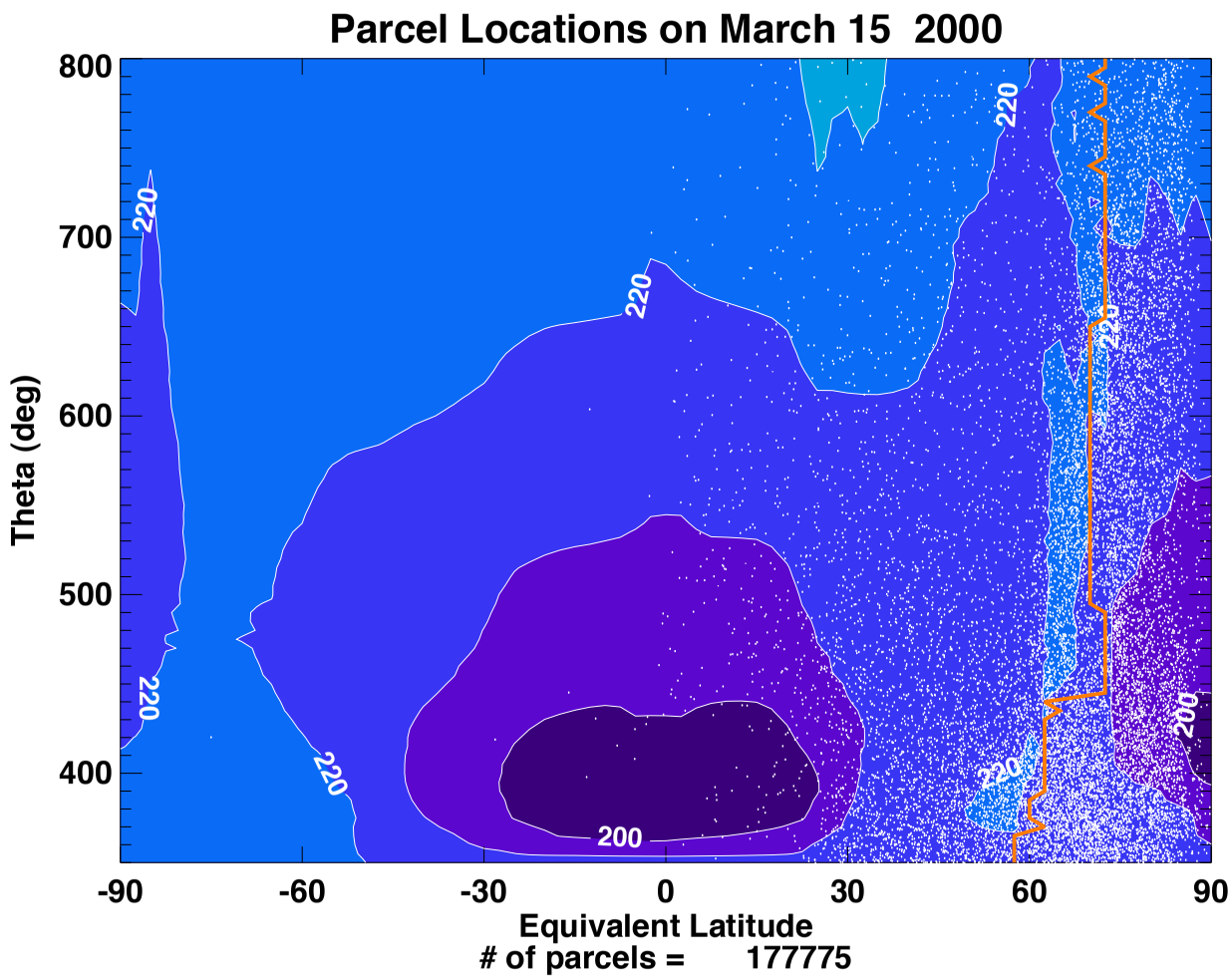
Parcel Locations on March 15 2000
Theta (deg)
800
700
600
500
400
-90
-60
-30
0
30
60
90
Equivalent Latitude
# of parcels = 177775
220
200

Figure 3

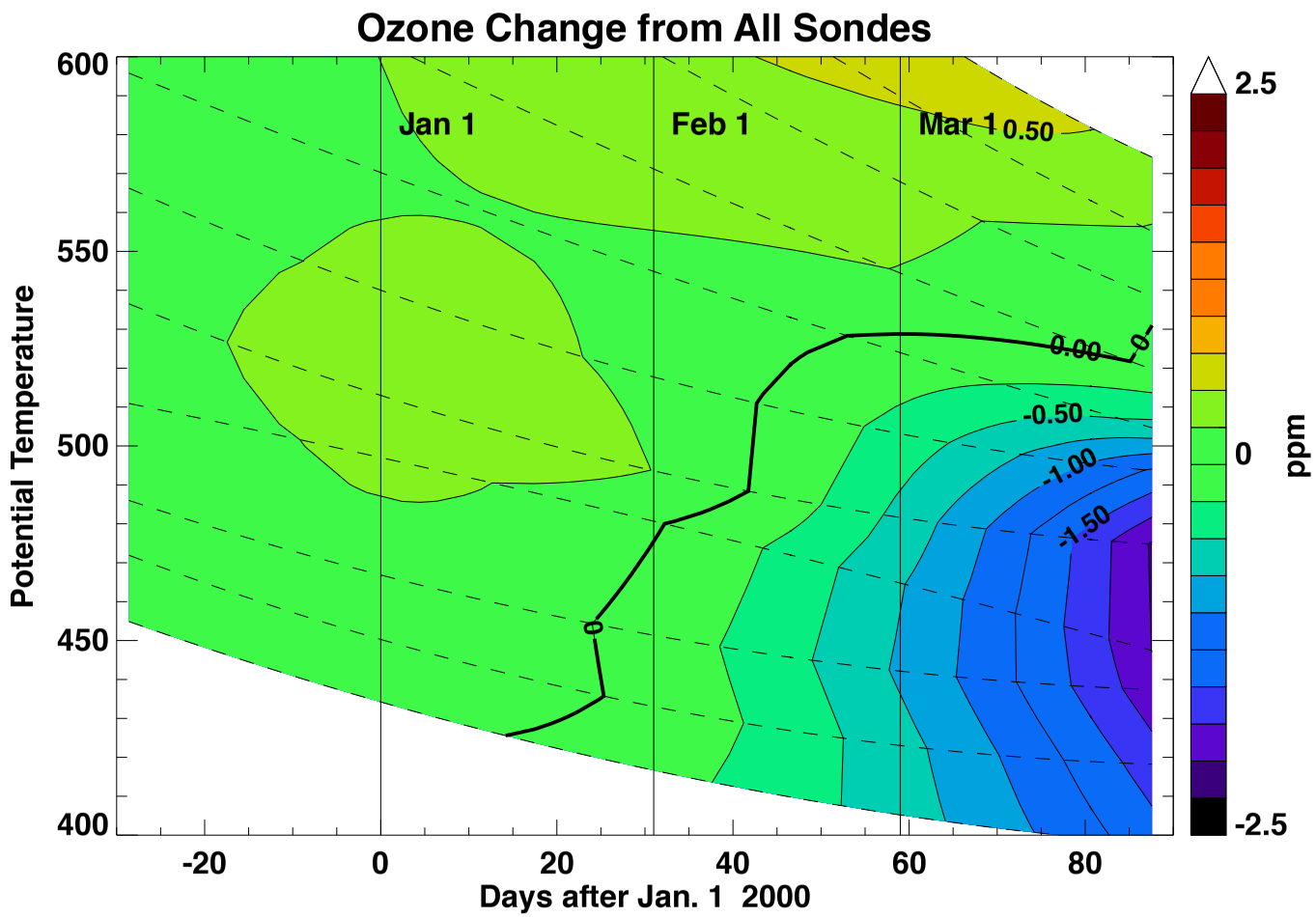
Ozone Change from All Sondes
Jan 1
Feb 1
Mar 1
0.50
0.00
0
-0.50
-1.00
-1.50
0
Potential Temperature
600
550
500
450
400
-20
0
20
40
60
80
Days after Jan. 1 2000
2.5
0
-2.5
ppm

Fig 4a

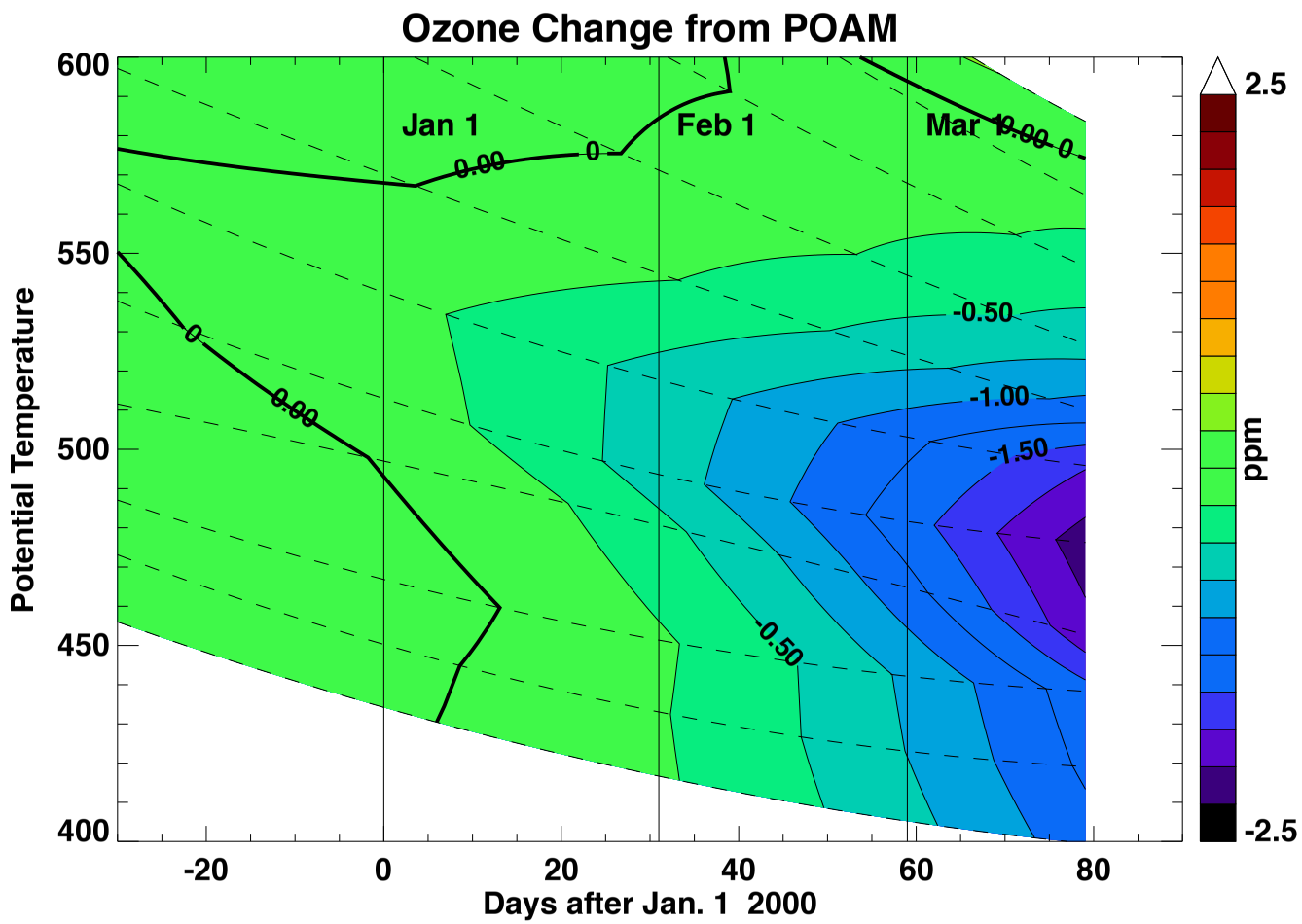
Ozone Change from POAM
Jan 1
Feb 1
Mar 1
0.00
0
-0.50
-1.00
-1.50
Potential Temperature
600
550
500
450
400
-20
0
20
40
60
80
Days after Jan. 1 2000
2.5
-2.5
ppm

Fig. 4b

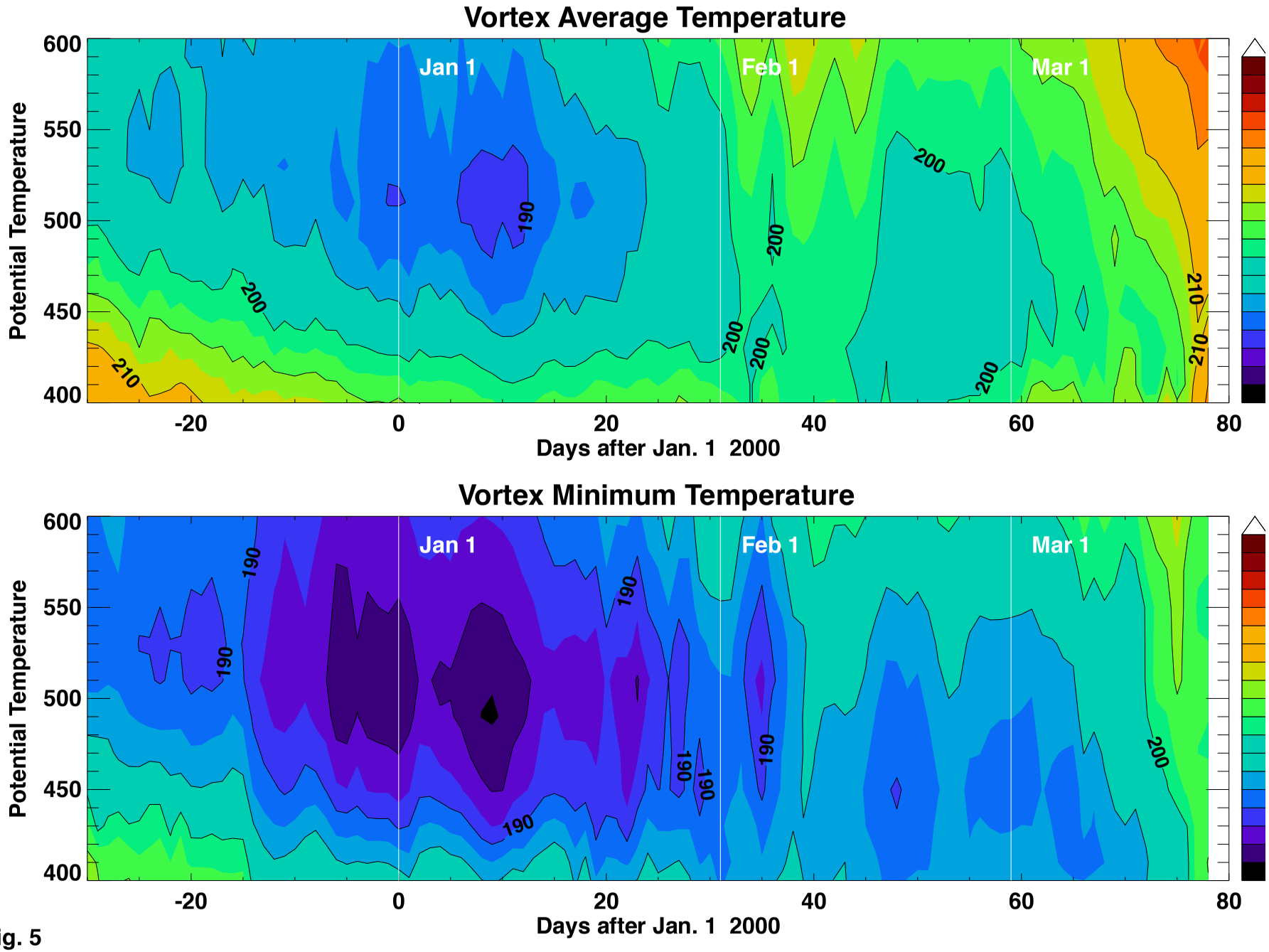
Vortex Average Temperature
Potential Temperature
600
550
500
450
400
Jan 1
Feb 1
Mar 1
190
200
210
-20
0
20
40
60
80
Days after Jan. 1 2000
Vortex Minimum Temperature
Potential Temperature
600
550
500
450
400
Jan 1
Feb 1
Mar 1
190
200
-20
0
20
40
60
80
Days after Jan. 1 2000

Fig. 5

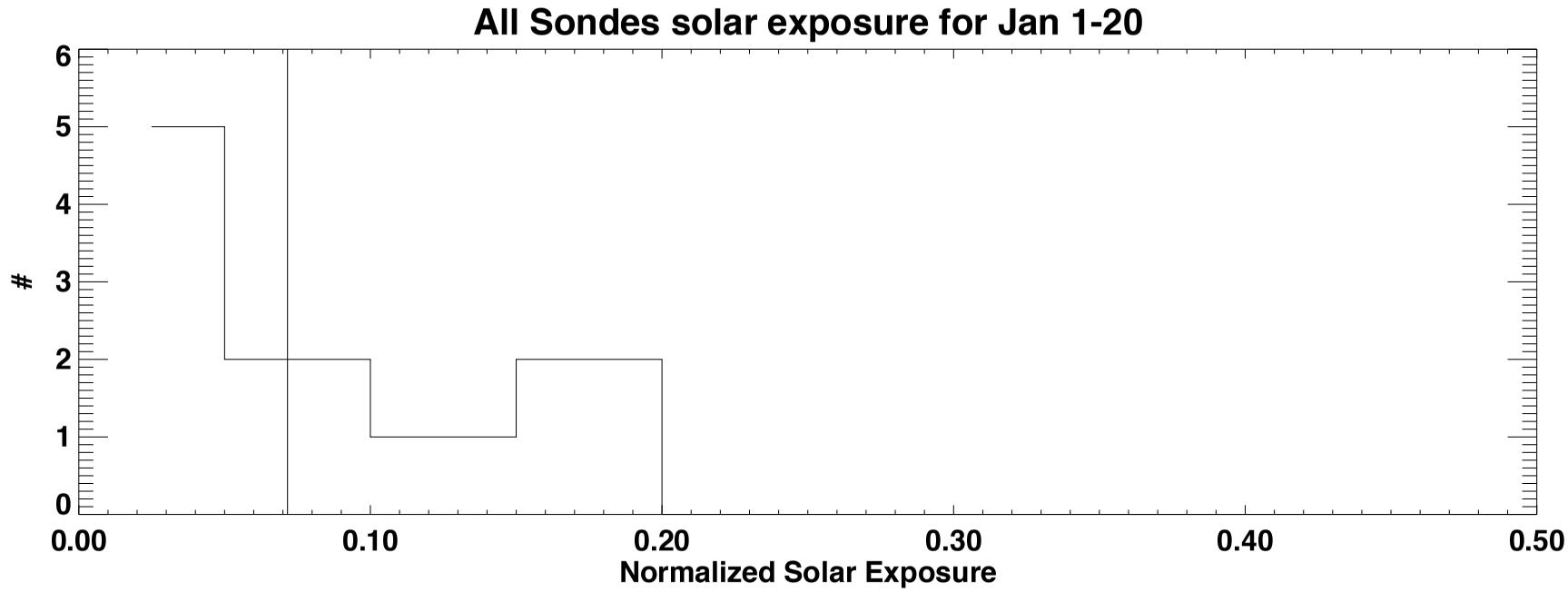
All Sondes solar exposure for Jan 1-20
#
0
1
2
3
4
5
6
0.00
0.10
0.20
0.30
0.40
0.50
Normalized Solar Exposure

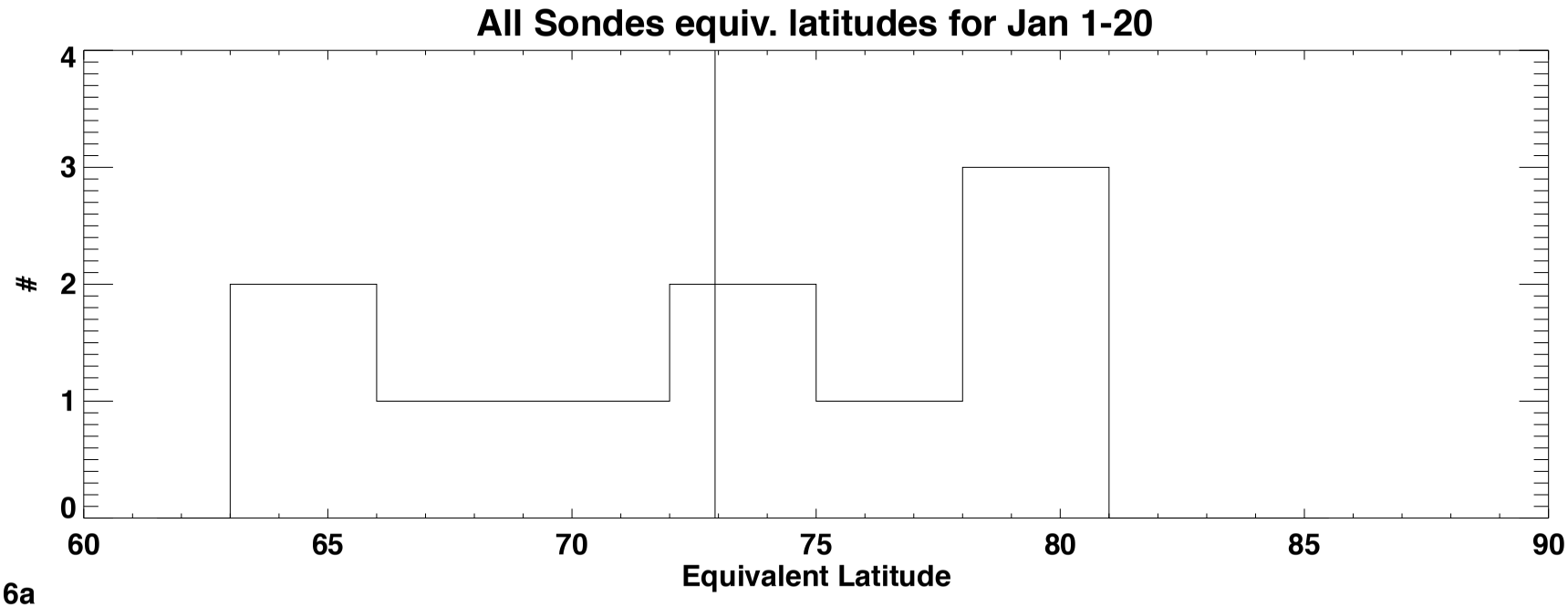
All Sondes equiv. latitudes for Jan 1-20
#
0
1
2
3
4
60
65
70
75
80
85
90
Equivalent Latitude

Fig. 6a

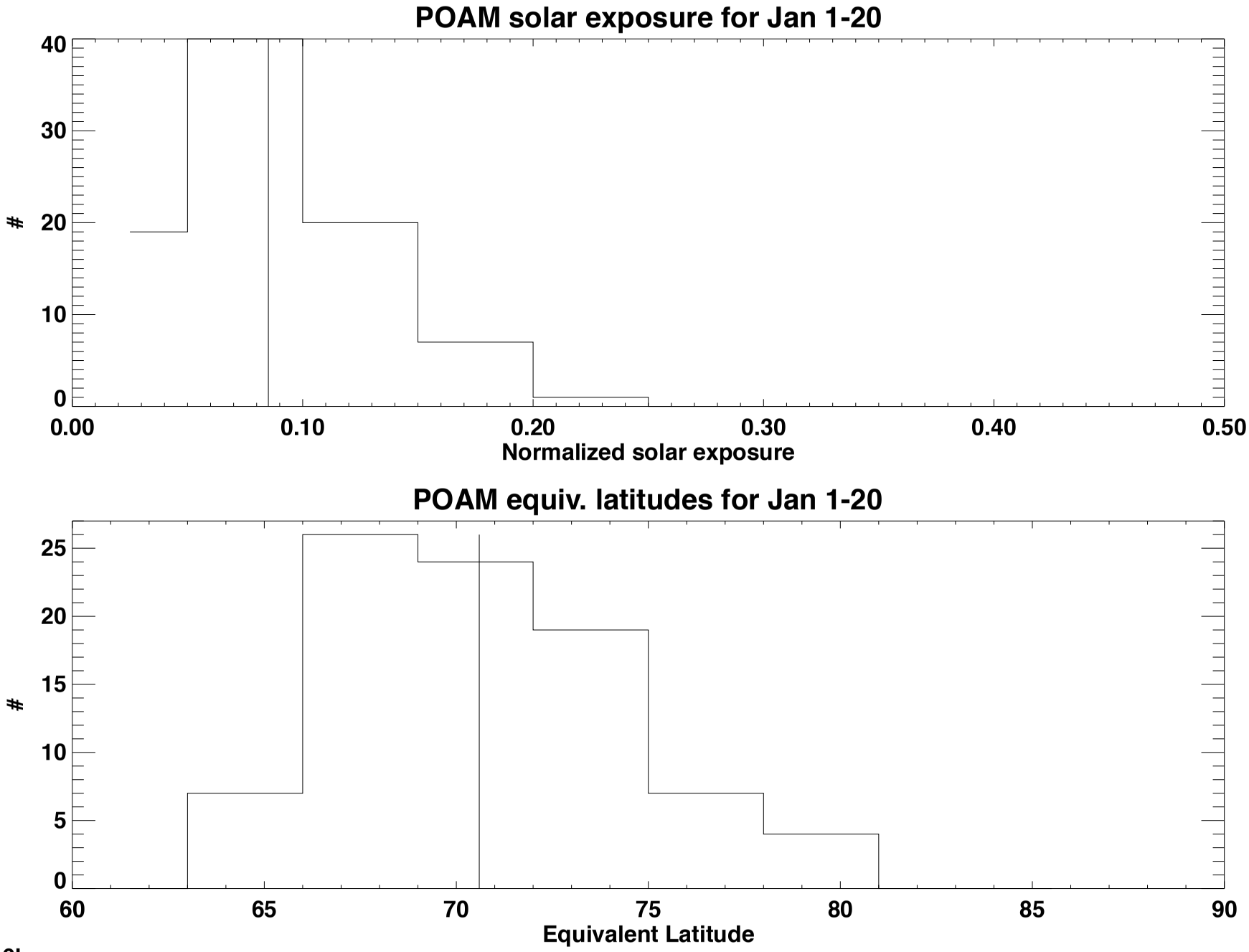
POAM solar exposure for Jan 1-20
#
0
10
20
30
40
0.00
0.10
0.20
0.30
0.40
0.50
Normalized solar exposure
POAM equiv. latitudes for Jan 1-20
#
0
5
10
15
20
25
60
65
70
75
80
85
90
Equivalent Latitude

Fig. 6b

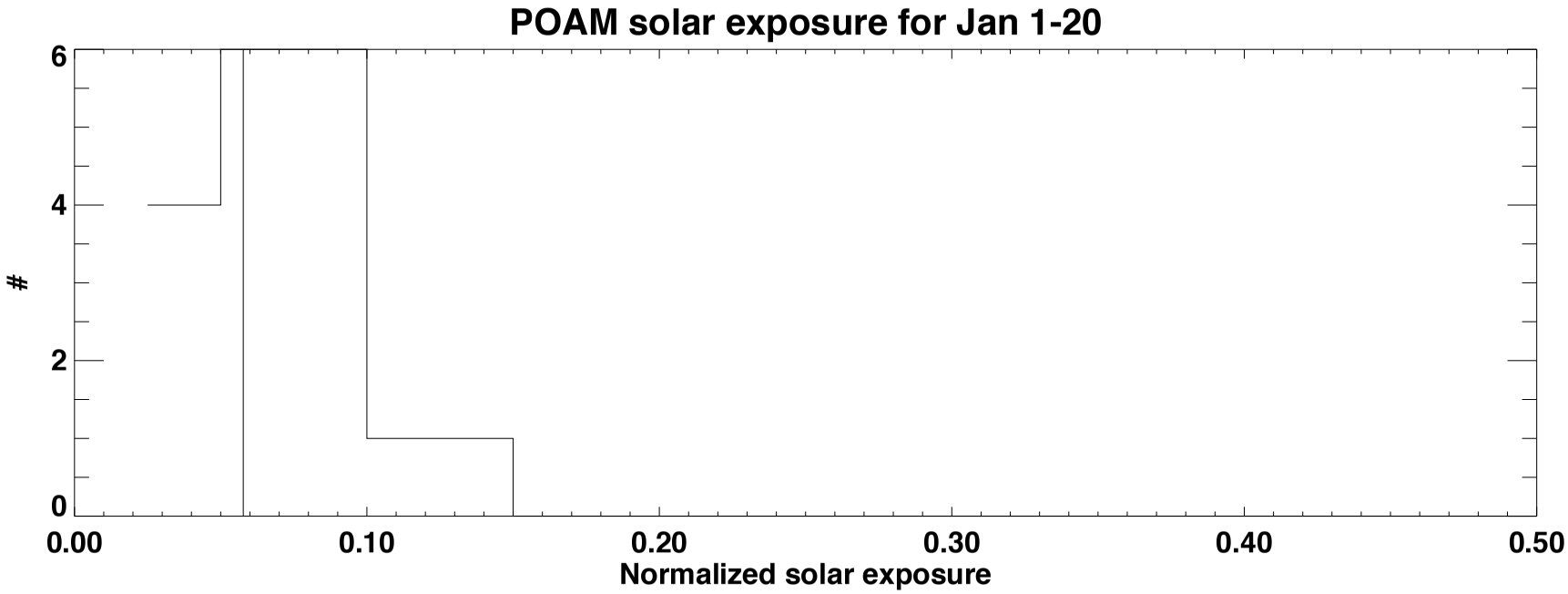
POAM solar exposure for Jan 1-20
#
0
2
4
6
0.00
0.10
0.20
0.30
0.40
0.50
Normalized solar exposure

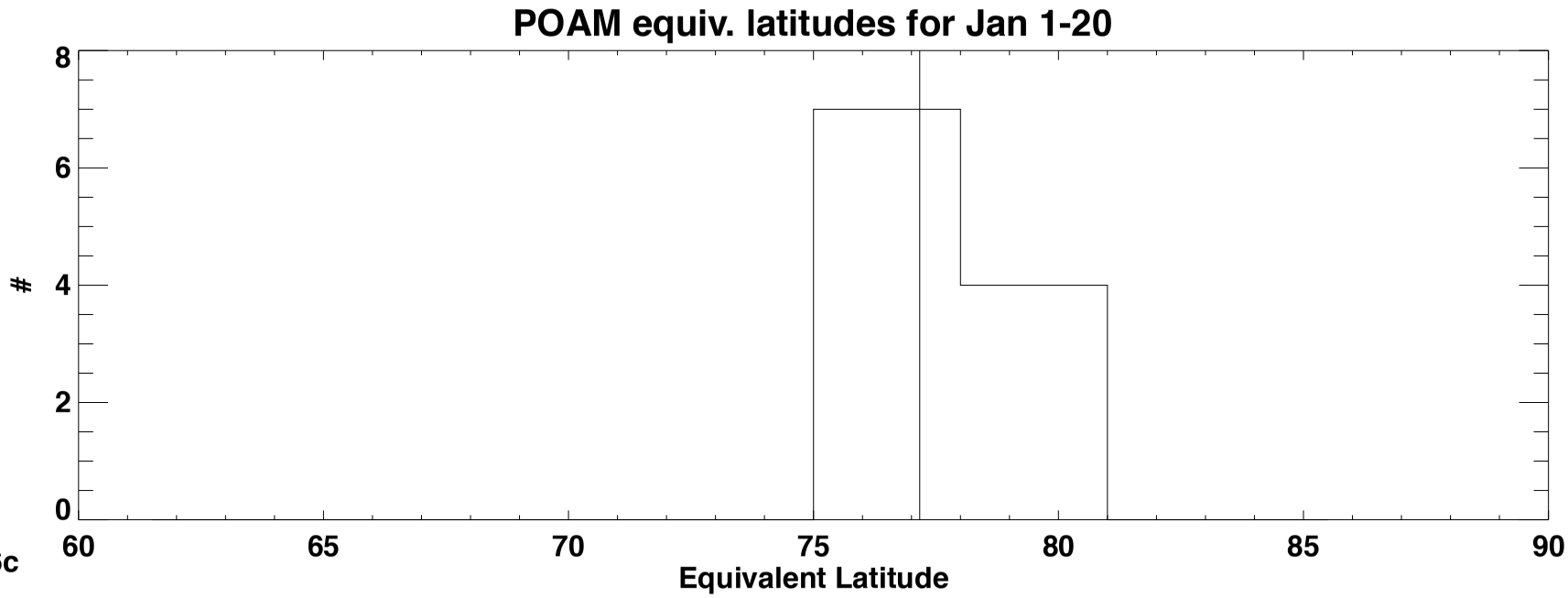
POAM equiv. latitudes for Jan 1-20
#
0
2
4
6
8
60
65
70
75
80
85
90
Equivalent Latitude

Fig 6c

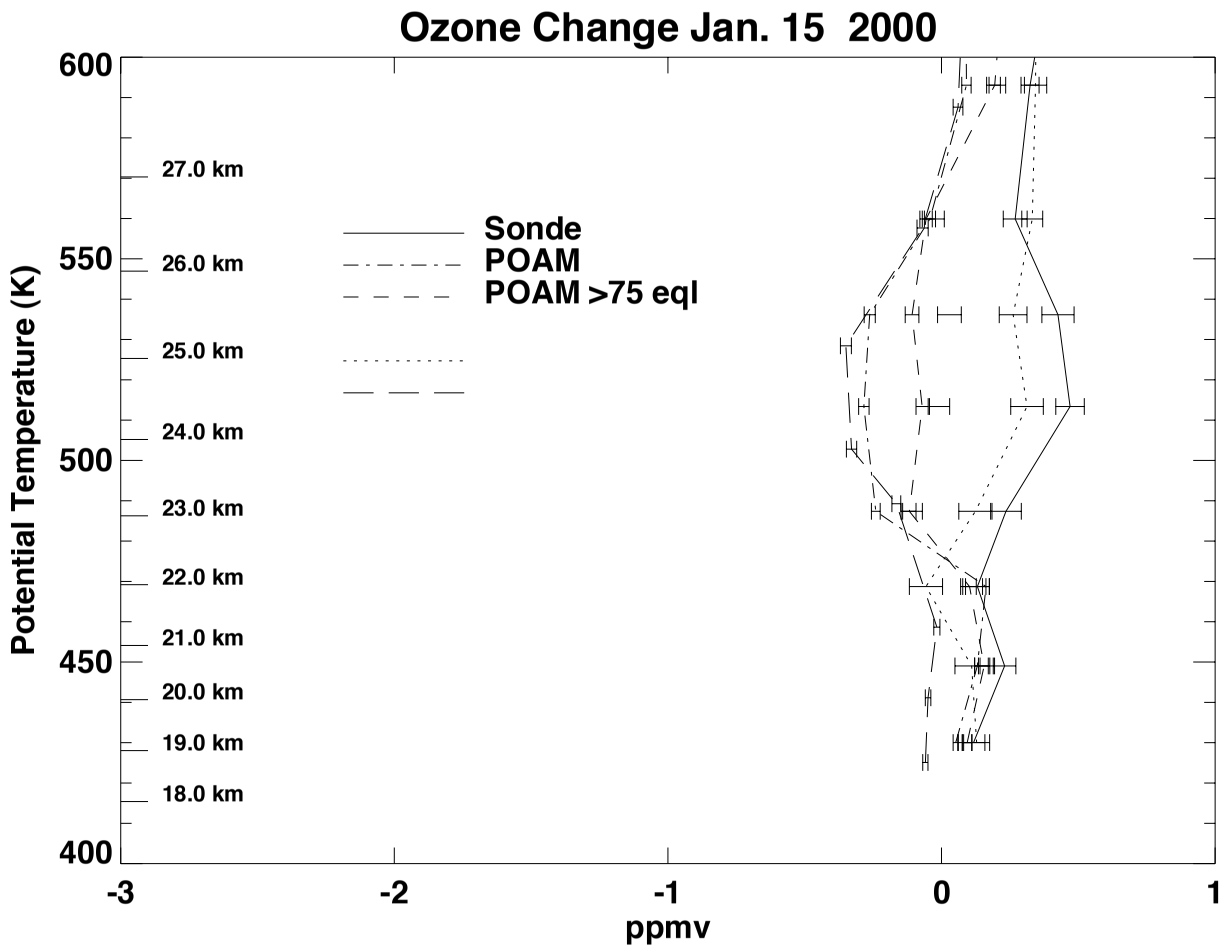
Ozone Change Jan. 15 2000
Potential Temperature (K)
600
550
500
450
400
27.0 km
26.0 km
25.0 km
24.0 km
23.0 km
22.0 km
21.0 km
20.0 km
19.0 km
18.0 km
Sonde
POAM
POAM >75 eql
-3
-2
-1
0
1
ppmv

Fig. 7

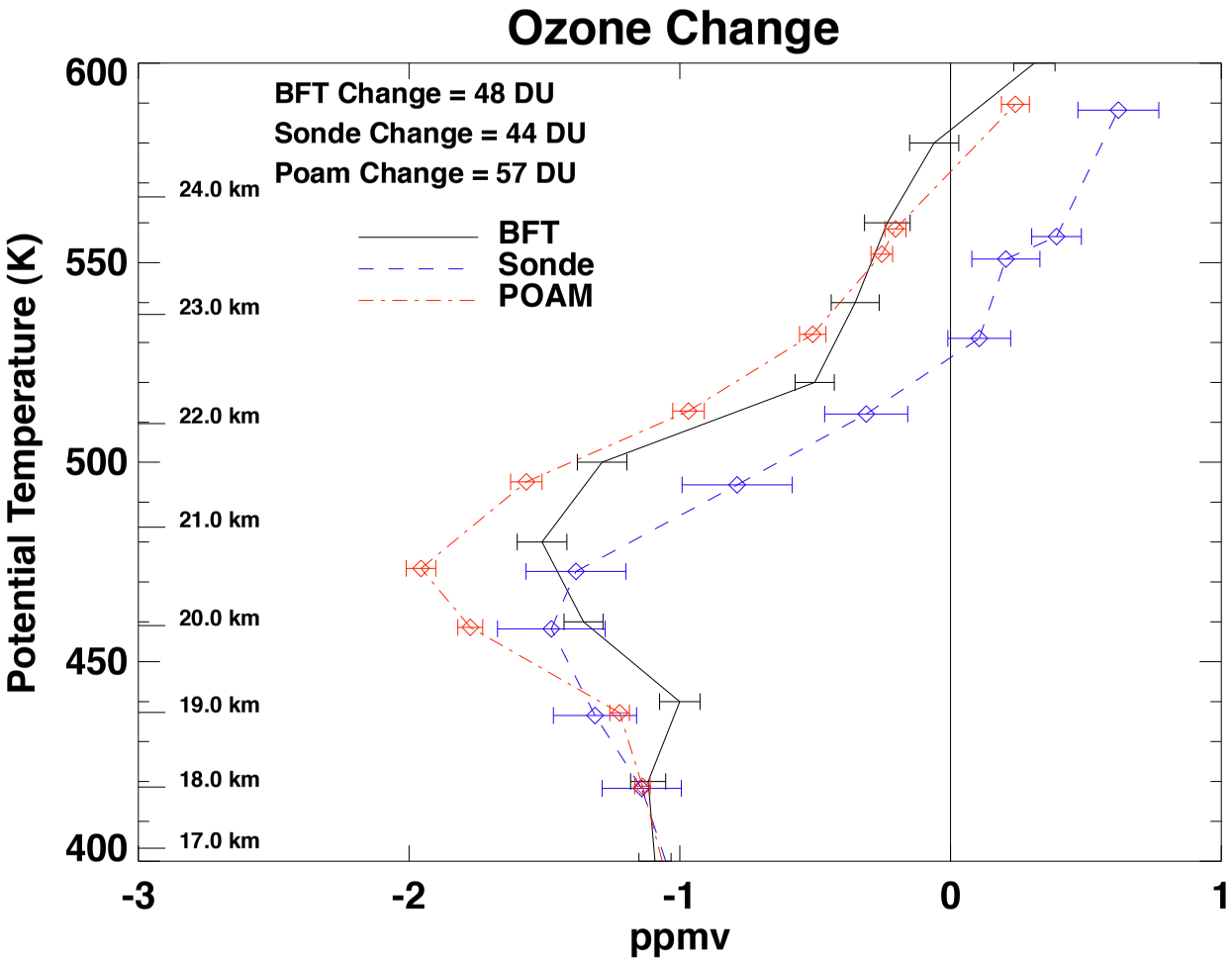
Ozone Change
BFT Change = 48 DU
Sonde Change = 44 DU
Poam Change = 57 DU
BFT
Sonde
POAM
24.0 km
23.0 km
22.0 km
21.0 km
20.0 km
19.0 km
18.0 km
17.0 km
Potential Temperature (K)
600
550
500
450
400
-3
-2
-1
0
1
ppmv

Fig 8

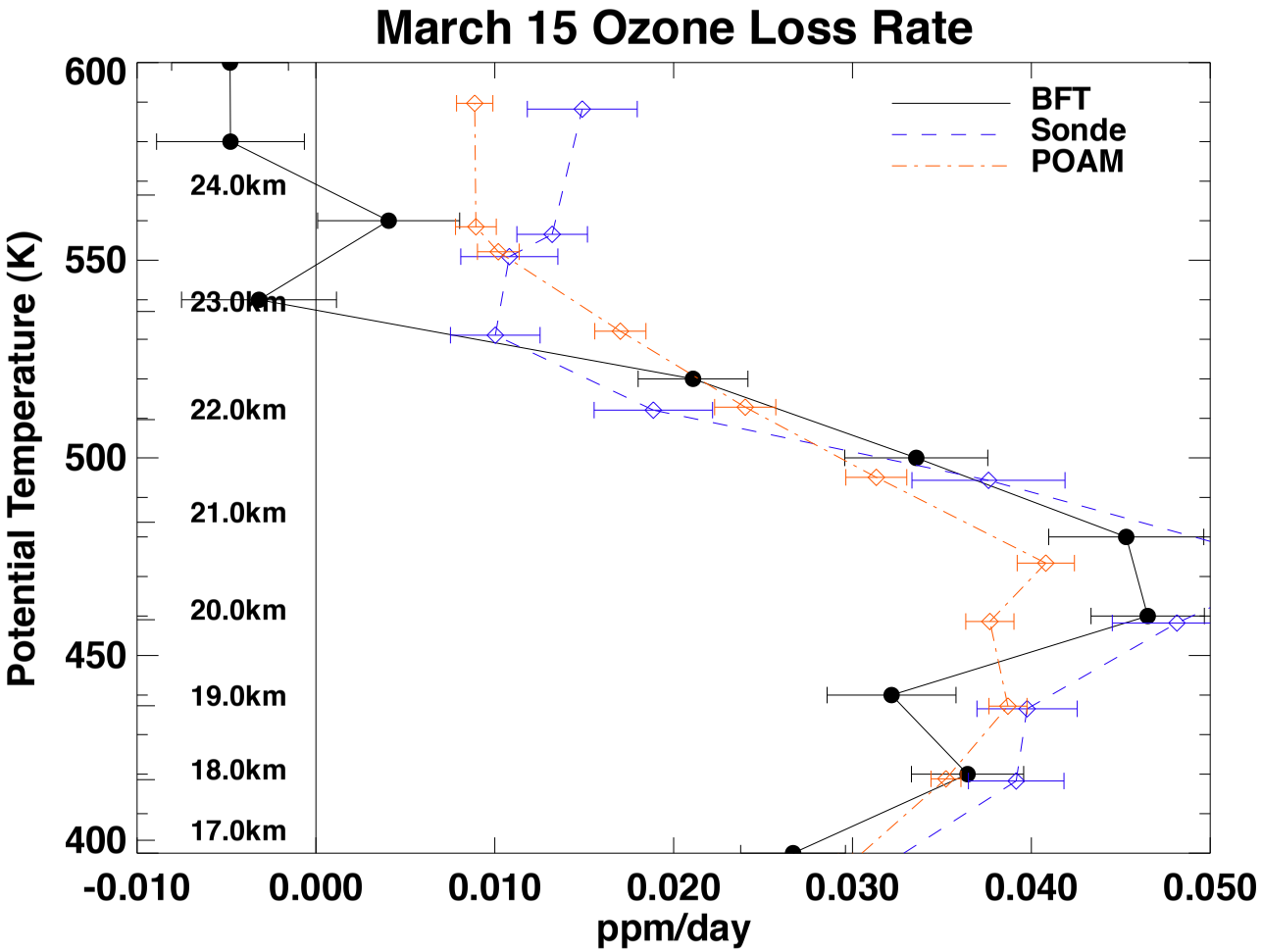
March 15 Ozone Loss Rate
BFT
Sonde
POAM
24.0km
23.0km
22.0km
21.0km
20.0km
19.0km
18.0km
17.0km
Potential Temperature (K)
600
550
500
450
400
-0.010
0.000
0.010
0.020
0.030
0.040
0.050
ppm/day

Fig. 9

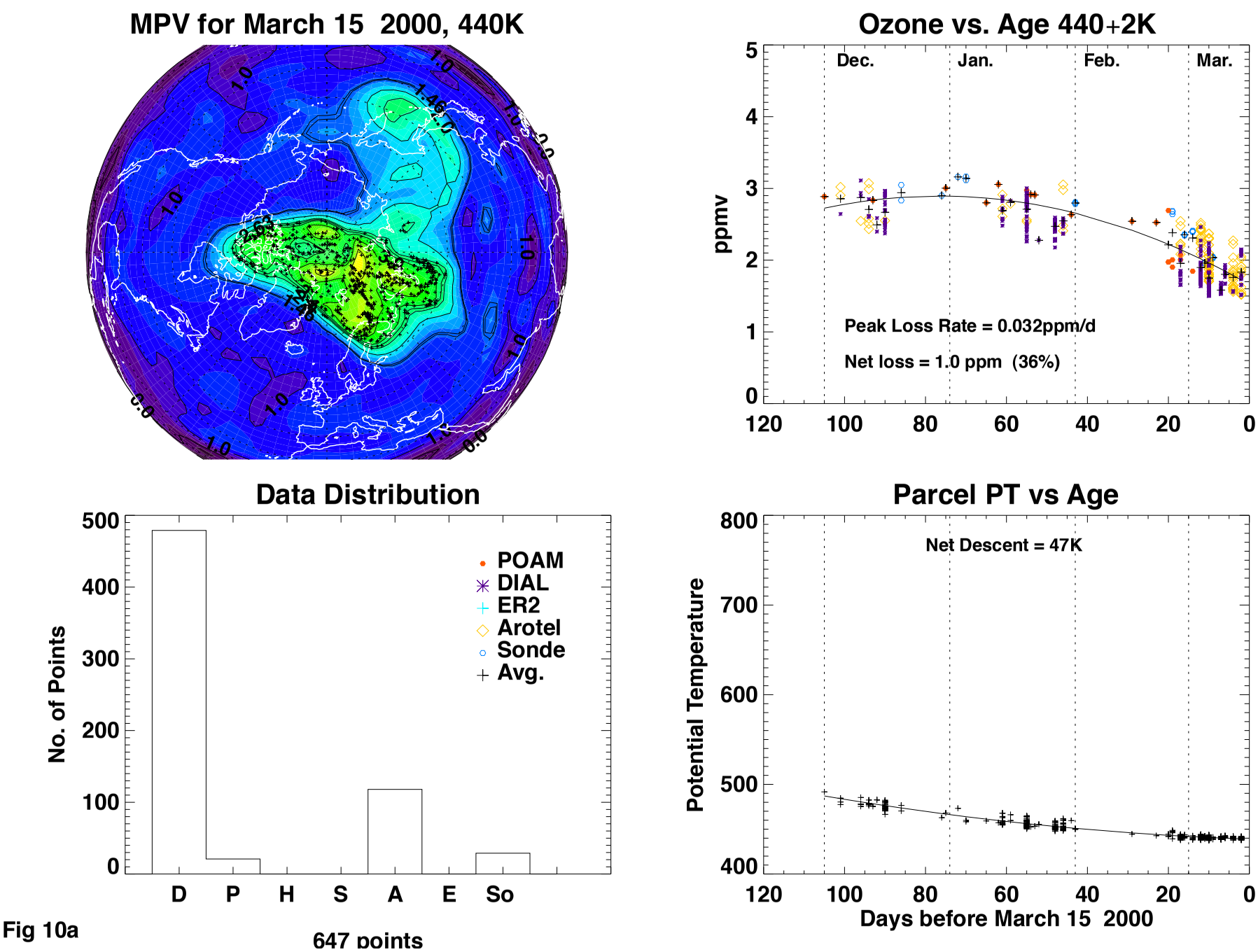
MPV for March 15 2000, 440K
Ozone vs. Age 440+2K
Dec.
Jan.
Feb.
Mar.
ppmv
Peak Loss Rate = 0.032ppm/d
Net loss = 1.0 ppm (36%)
Data Distribution
No. of Points
POAM
DIAL
ER2
Arotel
Sonde
Avg.
D
P
H
S
A
E
So
647 points
Parcel PT vs Age
Net Descent = 47K
Potential Temperature
Days before March 15 2000

Fig 10a

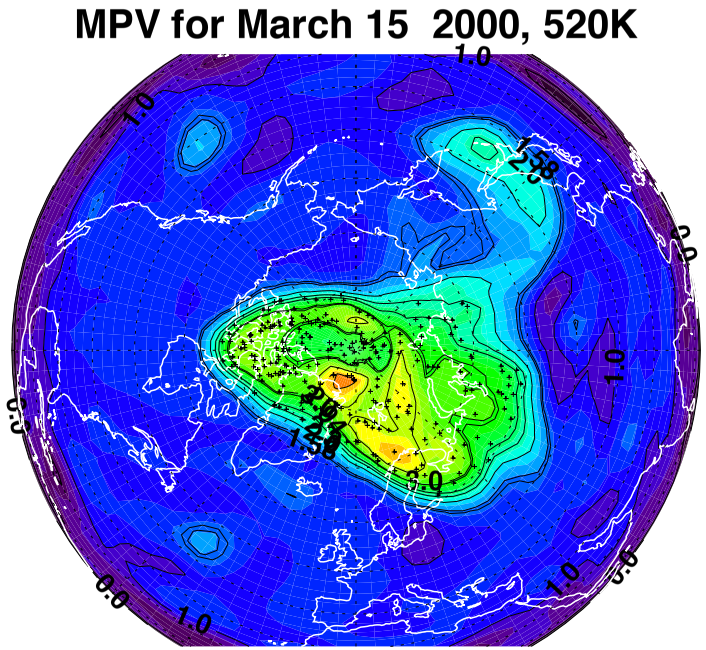
MPV for March 15 2000, 520K
1.0
0.0

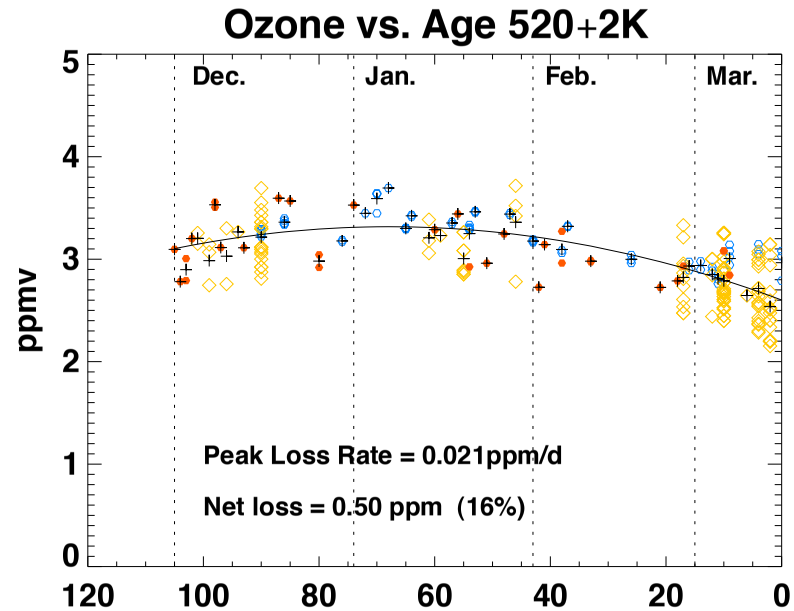
Ozone vs. Age 520+2K
Dec.
Jan.
Feb.
Mar.
ppmv
Peak Loss Rate = 0.021ppm/d
Net loss = 0.50 ppm (16%)
0
1
2
3
4
5
120
100
80
60
40
20
0

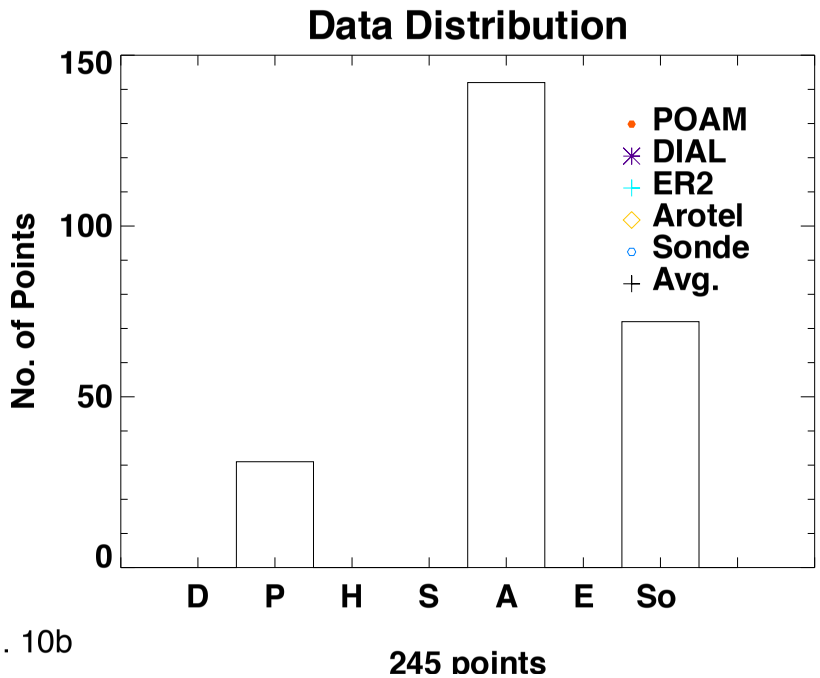
Data Distribution
No. of Points
0
50
100
150
POAM
DIAL
ER2
Arotel
Sonde
Avg.
D
P
H
S
A
E
So
245 points

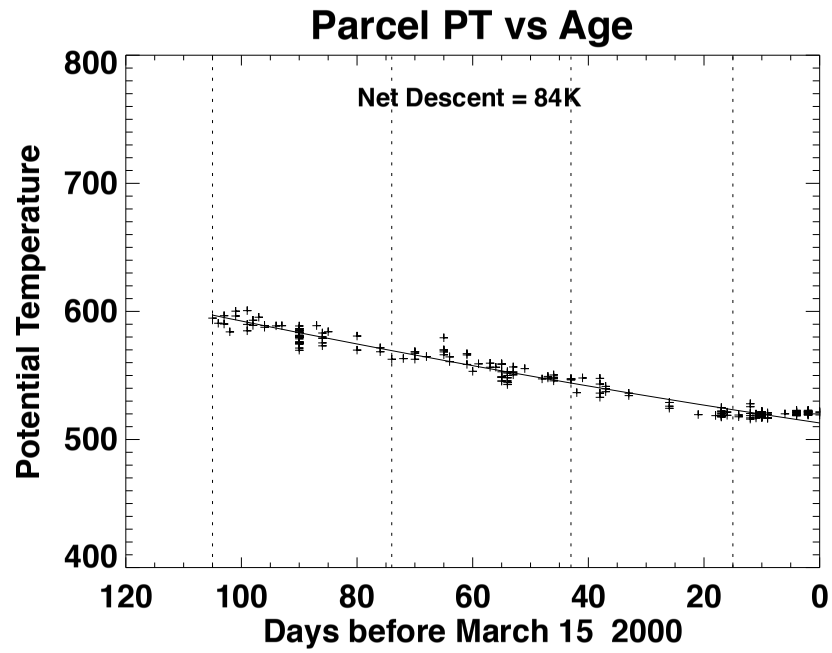
Parcel PT vs Age
Net Descent = 84K
Potential Temperature
400
500
600
700
800
120
100
80
60
40
20
0
Days before March 15 2000

Fig. 10b

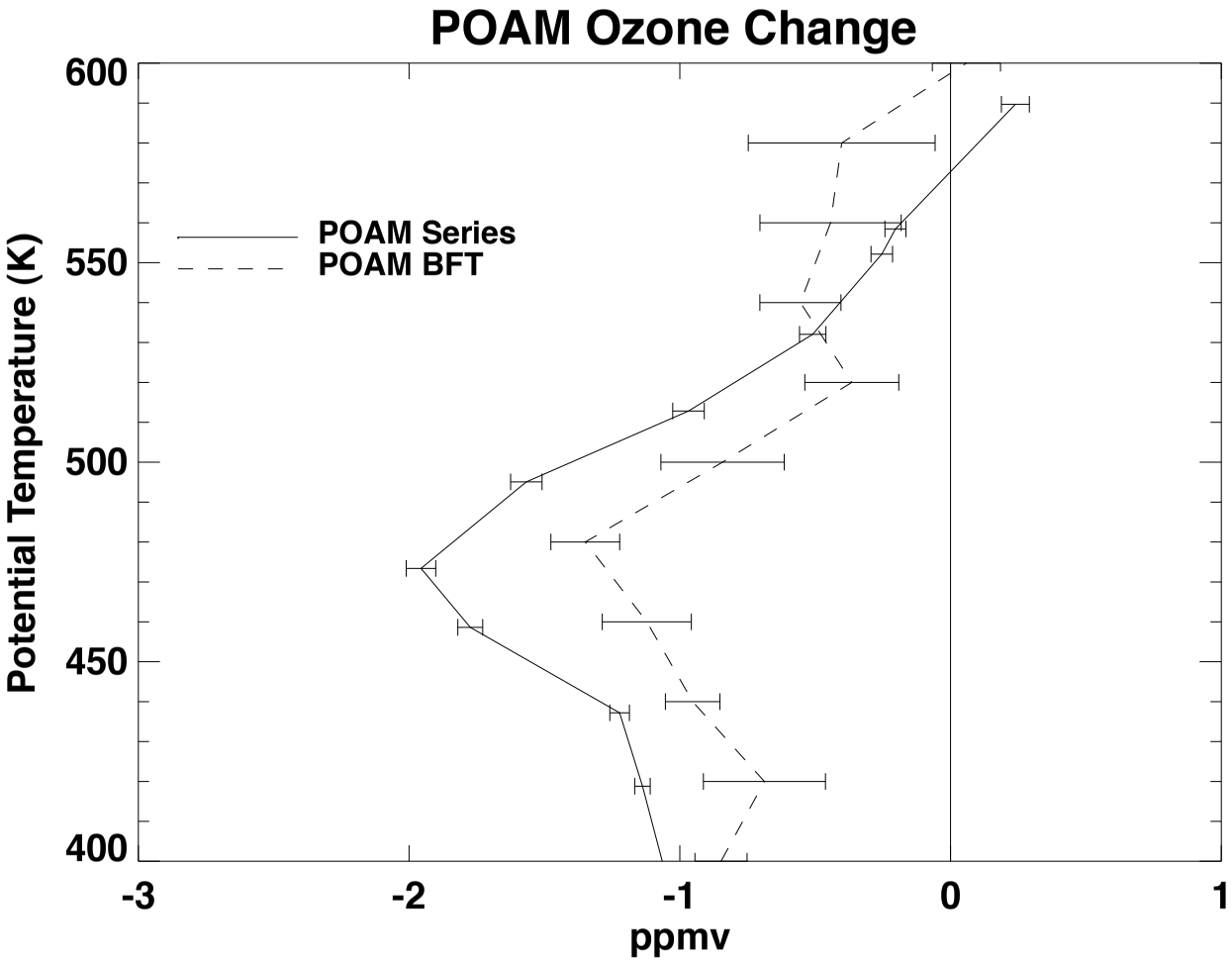
POAM Ozone Change
POAM Series
POAM BFT
Potential Temperature (K)
600
550
500
450
400
-3
-2
-1
0
1
ppmv

Fig. 11

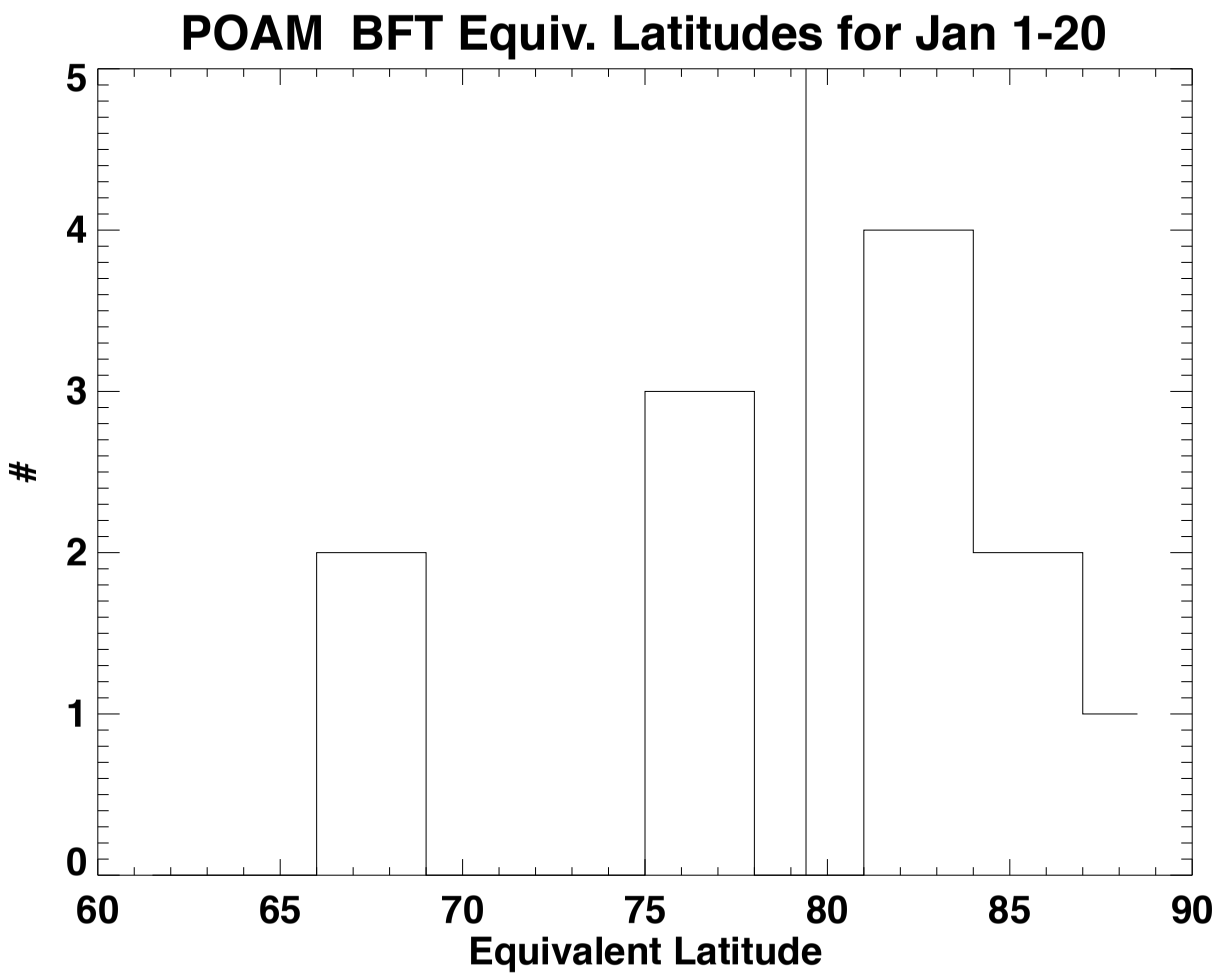
POAM BFT Equiv. Latitudes for Jan 1-20
#
0
1
2
3
4
5
60
65
70
75
80
85
90
Equivalent Latitude

Fig. 12

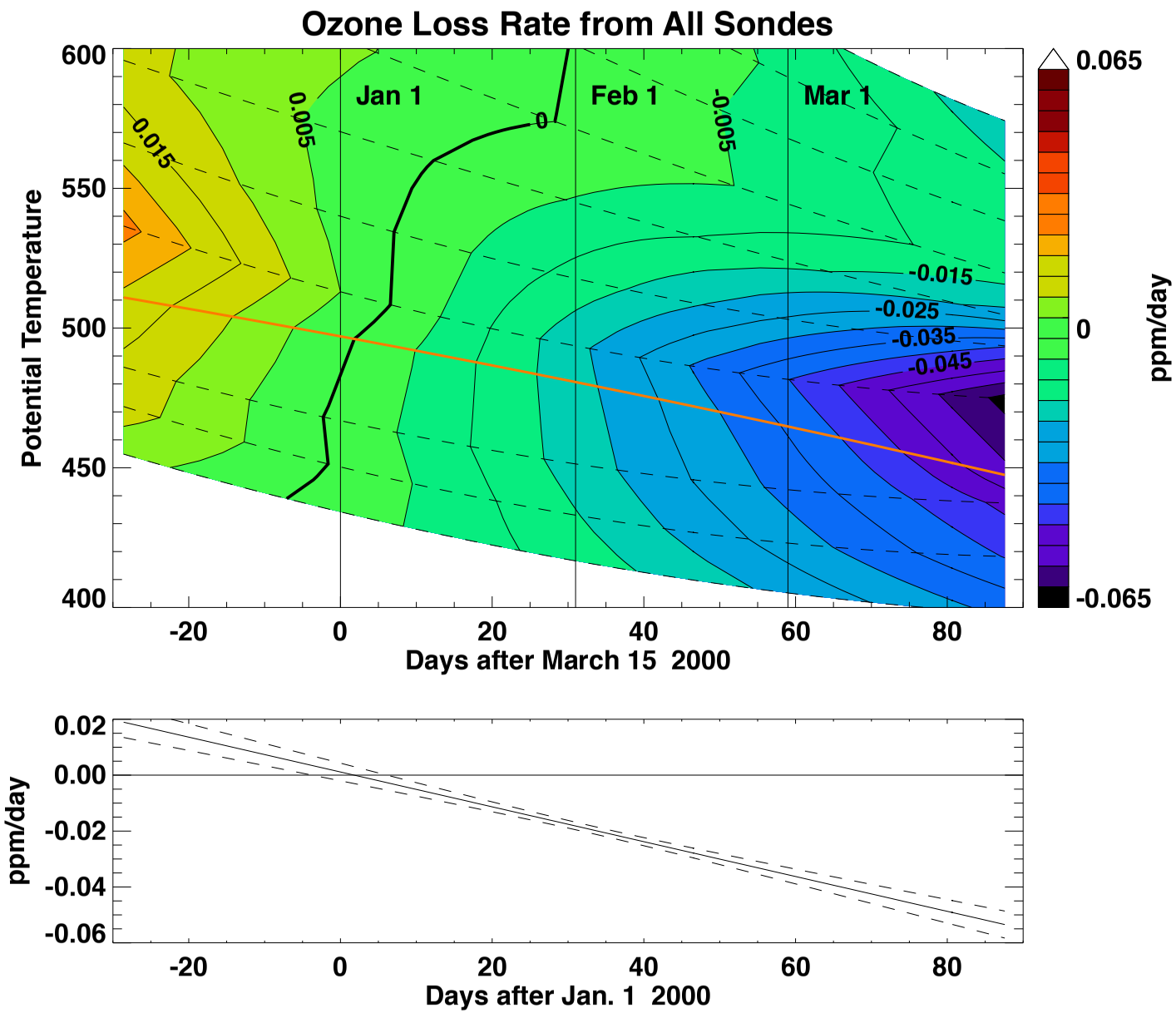
Ozone Loss Rate from All Sondes
Potential Temperature
600
550
500
450
400
Jan 1
Feb 1
Mar 1
0.015
0.005
0
-0.005
-0.015
-0.025
-0.035
-0.045
-20
0
20
40
60
80
Days after March 15 2000
0.065
0
-0.065
ppm/day
0.02
0.00
-0.02
-0.04
-0.06
ppm/day
Days after Jan. 1 2000

Fig. 13